Multiband Gutzwiller wave functions for general on-site interactions

J. Bünemann and W. Weber
Institut für Physik, Universität Dortmund, D-44221 Dortmund, Germany

F. Gebhard
Institut Laue-Langevin, Boîte Postale 156x, F-38042 Grenoble Cedex 9, France
(Received 22 October 1997)

We introduce Gutzwiller wave functions for multiband models with general on-site Coulomb interactions. As these wave functions employ correlators for the exact atomic eigenstates, they are exact both in the noninteracting and atomic limits. We evaluate them in infinite lattice dimensions for all interaction strengths without any restrictions on the structure of the Hamiltonian or the symmetry of the ground state. The results for the ground-state energy allow us to derive an effective one-electron Hamiltonian for Landau quasiparticles, applicable for finite temperatures and frequencies within the Fermi-liquid regime. As applications for a two-band model we study the Brinkman-Rice metal-to-insulator transition at half-band-filling, and the transition to itinerant ferromagnetism for two specific fillings, at and close to a peak in the density of states of the noninteracting system. Our results significantly differ from those for earlier Gutzwiller wave functions where only density-type interactions were included. When the correct spin symmetries for the two-electron states are taken into account, the importance of the Hund's-rule exchange interaction is even more pronounced, and leads to paramagnetic metallic ground states with large local magnetic moments. Ferromagnetism requires fairly large interaction strengths, and the resulting ferromagnetic state is a strongly correlated metal. [S0163-1829(98)02212-7]

I. INTRODUCTION

In transition metals and their compounds the electrons of the open *d* shells participate in the itineracy of the valence electrons. At the same time their atomic correlations, as described, e.g., by Hund's first and second rules, remain important. The competition between the electrons' itinerant and local features results in many interesting phenomena: magnetism is most prominent, but metal-to-insulator transitions, high-to-low-spin changes, orbital ordering etc. also occur in these materials.

For insulating compounds it is commonly accepted that their magnetic behavior can be described in terms of the spins of *localized* electrons which are coupled by superexchange via the ligands. However, there are conflicting views on the magnetism of the metallic state. One line of reasoning which dates back to van Vleck and others assumes rather small charge fluctuations around the average (atomic) d^n configuration, and the localized spins also remain a useful concept in the metallic state (minimum polarity model[1]). The other school, starting from the Hartree-Fock-Stoner theory, treats magnetism within a single-particle band theory, i.e., in a completely itinerant limit. In particular, spin-density-functional theory quite successfully describes the ferromagnetism of the iron group metals, not only concerning magnetic moments but also such details as the shapes of complicated multisheet Fermi surfaces.[2] In the spirit of a free-electron theory the spin-density-functional theory generally assumes a local exchange-correlation potential which is a function of the local charge and spin densities. The success of this effective single-particle theory is quite surprising since, in the atomic limit, it cannot reproduce the open-shell electronic structure.

In his seminal work, Gutzwiller[3] proposed a variational approach to the problem of itinerant ferromagnetism in the Hubbard model.[4] In his many-body trial state atomic configurations with large deviations from the average occupancy could be reduced with respect to a Hartree-Fock reference state, depending on the value of the variational parameter. Therefore, his approach incorporated both the itinerant and localized aspects of itinerant magnetism. Gutzwiller introduced an approximate evaluation of his many-body wave function, the so-called Gutzwiller approximation, and concluded from his one-band results that itinerant ferromagnetism requires large interaction strengths. Later, Brinkman and Rice realized[5] that the Gutzwiller approximation contained a transition from a paramagnetic metal to a paramagnetic insulator in which all electrons are localized. The Brinkman-Rice insulator provides an instructive example for the more general class of Mott-Hubbard insulators.[6,7]

During the last decade, analytical techniques were developed which allow for an exact evaluation of the single-band Gutzwiller wave function in one dimension,[8] and in the limit of infinite dimensions.[9,10] For the latter case the results of the Gutzwiller approximation were found to become exact. Furthermore, the results of the Kotliar-Ruckenstein slave-boson mean-field theory[11] were rederived for the paramagnetic and antiferromagnetic cases.[9,10] In this work we extend the single-band formalism of Refs. 12 and 13, which provided exact results in infinite dimensions for the whole class of Gutzwiller wave functions. For the one-band case the Gutzwiller variational approach in infinite dimensions and slave-boson theories[11,14] on a mean-field level were shown to be completely equivalent; see Ref. 7 for a recent review.

The case of multiband systems poses a more complicated problem. Each lattice site represents an atom with an incom-

pletely filled shell. Consequently, the atomic Hamiltonian $\hat{H}_{\rm at}$ should include the relevant properties of the electronic structure of isolated atoms or ions. This means that it should comply with Hund's first rule, it should reproduce the essential features of low-lying multiplet excitations, and it has to incorporate the symmetry of the ligand field. The commonly used form for the atomic part $\hat{H}_{\rm at}$ of the multiband Hubbard Hamiltonian includes (i) an orbital-diagonal density-density interaction of strength U as in the single-band case, and an orbital-nondiagonal density-density interaction of strength U'; and (ii) two-particle spin-exchange terms of strength J such that the ground state of $\hat{H}_{\rm at}$ fulfills Hund's first rule, i.e., it exhibits maximum spin for $J>0$. Frequently, the spin-exchange terms are taken only partially into account. If the (orbital) spin-flip terms are neglected, we are left with $\hat{H}_{\rm at}^{\rm dens}$ which contains only density-density interactions on the atomic sites.

It should be noted that a while ago atomic Hamiltonians similar to $\hat{H}_{\rm at}$ were studied using the ''local ansatz,''[15,16] a scheme in the spirit of the Gutzwiller method. However, the results presented were limited to small interaction strengths. Recently, the Gutzwiller method was generalized to treat multiband Hubbard models with local-density-type interactions $\hat{H}_{\rm at}^{\rm dens}$ of arbitrary strengths.[17–20] The essential idea was to evaluate correlators for atomic multielectron configurations made up of spin-orbital product states (''Slater determinants''). This was possible since $\hat{H}_{\rm at}^{\rm dens}$ is diagonal in these configurations. In a first step the Gutzwiller approximation was used;[17–19] later it was shown that these results become exact in the limit of infinite dimensions.[20] In Ref. 20 we compared our results with those of previous generalizations of the Gutzwiller approximation to the case of degenerate bands.

However, the frequently used treatment of $\hat{H}_{\rm at}$, as discussed above, still *violates* the atomic symmetry; for an example, see below. The reason is the incomplete form of the exchange interaction. To establish the correct symmetry it is necessary to include *all* exchange terms which result from a (spin conserving) two-particle interaction, i.e., we will have to consider the contributions from up to four different spin orbits. Then the proper $\mathfrak{n}$-electron atomic eigenstates are certain linear combinations of the respective $\mathfrak{n}$-electron spin-orbit product configurations. As a consequence, the optimum way to generalize the Gutzwiller wave function to multiband systems is the use of correlators for the atomic $\mathfrak{n}$-electron eigenstates instead of the pure spin-orbit product states.

In this paper we introduce and evaluate such variational wave functions with atomic correlations. Our formulation allows for arbitrary orbital bases, including more than one orbital type per representation, i.e., more than one type of s, p, or d orbitals. It also allows for an arbitrary number of atomic sites in the unit cell. In the limit of infinite dimension, exact results for the ground-state energy are given in terms of an effective single-particle Hamiltonian which defines the band structure of correlated electrons. Thus our theory naturally extends to finite temperatures (Fermi-liquid regime). As an example we apply our theory to a two-band model, and show that the correct treatment of the atomic correlations yields a variety of results which quantitatively and, in some cases, even qualitatively differ from those using pure density correlations.

Our paper is structured as follows. In Sec. II we introduce the multiband Hubbard Hamiltonian with purely on-site interactions. The spectrum of the general atomic Hamiltonian is supposed to be known. Then, in Sec. III, we specify the class of Gutzwiller wave functions with atomic correlations, and give the exact results for the ground-state energy in infinite dimensions. For the case of pure density correlations we recover our previous expressions.[17,18,20] In Sec. IV, we discuss the example of two partly filled e_g bands in more detail. We study the Brinkman-Rice metal-insulator transition at half-band-filling, and itinerant ferromagnetism for two generic band fillings. A summary and conclusions close our presentation. Technical details are deferred to the Appendix.

II. HAMILTON OPERATOR

A. Multiband Hubbard model

Our multiband Hubbard model[4] is defined by the Hamiltonian

$$\hat{H}=\sum_{i,j;\boldsymbol{\sigma},\boldsymbol{\sigma}'} t_{i,j}^{\boldsymbol{\sigma},\boldsymbol{\sigma}'}\hat{c}_{i;\boldsymbol{\sigma}}^{+}\hat{c}_{j;\boldsymbol{\sigma}'}+\sum_{i}\hat{H}_{i;\rm at}\equiv\hat{H}_1+\hat{H}_{\rm at}. \qquad (1)$$

Here, $\hat{c}_{i;\boldsymbol{\sigma}}^{+}$ creates an electron with combined spin-orbit index $\boldsymbol{\sigma}=1,\ldots,2N$ ($N=5$ for $3d$ electrons) at the lattice site i of a solid. We do not yet specify a periodic lattice, i.e., the sites i may also represent ligand atoms. Therefore, the number of orbitals N also depends on the site, $N\equiv N_i$. To keep the notation transparent we will drop this additional index in the following, and we will use the notion ''orbital'' for spin-orbit states.

The first term in Eq. (1), $\hat{H}_1$, represents an appropriate single-particle tight-binding Hamiltonian. Crystal-field terms are included in the orbital energies $t_{i,i}^{\boldsymbol{\sigma},\boldsymbol{\sigma}}\equiv\epsilon_{i;\boldsymbol{\sigma}}$. We may also allow nondiagonal crystal-field terms $t_{i,i}^{\boldsymbol{\sigma},\boldsymbol{\sigma}'}$ for $\boldsymbol{\sigma}\neq\boldsymbol{\sigma}'$ in case of a sufficiently large orbital basis (or a sufficiently low atomic-site symmetry). In this paper we do not include spin-orbit coupling, and we may therefore assume that the terms $t_{i,j}^{\boldsymbol{\sigma},\boldsymbol{\sigma}'}$ are spin-independent quantities which only depend on the spatial part of the underlying spin-orbit wave functions.

In model (1) we assume that the electrons interact only locally. Separating the density-density interactions we may write the atomic Hamiltonian as two terms,

$$\hat{H}_{i;\rm at}=\sum_{\boldsymbol{\sigma},\boldsymbol{\sigma}'(\boldsymbol{\sigma}\neq\boldsymbol{\sigma}')}\mathcal{U}_i^{\boldsymbol{\sigma},\boldsymbol{\sigma}'}\hat{n}_{i;\boldsymbol{\sigma}}\hat{n}_{i;\boldsymbol{\sigma}'}+\sum_{(\boldsymbol{\sigma}_1<\boldsymbol{\sigma}_2)\neq(\boldsymbol{\sigma}_3>\boldsymbol{\sigma}_4)}\mathcal{J}_i^{\boldsymbol{\sigma}_1,\boldsymbol{\sigma}_2;\boldsymbol{\sigma}_3,\boldsymbol{\sigma}_4}\hat{c}_{i;\boldsymbol{\sigma}_1}^{+}\hat{c}_{i;\boldsymbol{\sigma}_2}^{+}\hat{c}_{i;\boldsymbol{\sigma}_3}\hat{c}_{i;\boldsymbol{\sigma}_4}. \qquad (2)$$

The exchange-type second term transfers two electrons from the orbitals $\boldsymbol{\sigma}_3>\boldsymbol{\sigma}_4$ into the orbitals $\boldsymbol{\sigma}_1<\boldsymbol{\sigma}_2$. The quantities $\mathcal{U}_i$ and $\mathcal{J}_i$ represent all possible two-particle (Coulomb) interactions compatible with the symmetry at site i.

B. Atomic problem

In our variational wave functions we will deal with operators which project onto atomic $\mathfrak{n}$-electron eigenstates $|\Gamma_i\rangle$ with arbitrary number $0 \leqslant \mathfrak{n} \leqslant 2N$. Altogether we will have 2^{2N} eigenstates. Each of these $\mathfrak{n}$-electron eigenstates has the proper symmetry, i.e., they can be classified according to irreducible representations of the group defined by the symmetry of site i. Part of this classification is according to the total spin quantum number as $\hat{H}_{i;\mathrm{at}}$ commutes with $(\vec{S}_i)^2$. The problem of classification is treated in detail by many authors;[21,22] here we refer to Ref. 23.

We now suppress the site index, and introduce the following notation for all possible 2^{2N} multiorbital configurations I and the corresponding multielectron configuration states $|I\rangle$.

(1) A configuration I is characterized by the electron occupation of the orbitals,

$$I \in \{\varnothing;(1),\ldots,(2N);(1,2),\ldots,(2,3),\ldots(2N-1,2N);\ldots;(1,\ldots,2N)\}. \tag{3}$$

Here the symbol $\varnothing$ in Eq. (3) means that the site is empty. Then, there follow all $2N$ one-electron configurations, all $N(2N-1)$ two-electron configurations—the sequence of numbers in round brackets $(\boldsymbol{\sigma}_1,\boldsymbol{\sigma}_2,\ldots)$ is irrelevant—and so on up to the $2N$ electron configuration $(1,\ldots,2N)$. For example, $(\boldsymbol{\sigma}_1,\boldsymbol{\sigma}_2)$ specifies one of the 45 possible $[\mathrm{Ar}]3d^2$ configurations of a Ti^{2+} ion in the frozen-core approximation.

In general, we interpret the indices I in Eq. (3) as sets in the usual sense. For example, in the atomic configuration $I \setminus I'$ only those orbitals in I are occupied which are not in I'. The complement of I is $\overline{I} = (1,2,\ldots,2N) \setminus I$, i.e., in the atomic configuration $\overline{I}$ all orbitals but those in I are occupied.

(2) $|I| \equiv \mathfrak{n}$, i.e., the absolute value $|I|$ of a configuration indicates the number $\mathfrak{n}$ of a multielectron state,

$$|\varnothing| = 0; |(\boldsymbol{\sigma}_1)| = 1; |(\boldsymbol{\sigma}_1,\boldsymbol{\sigma}_2)| = 2; \ldots; |(1,\ldots,2N)| = 2N. \tag{4}$$

(3) A multielectron configuration state (Slater determinant) is constructed as

$$|I\rangle = |\boldsymbol{\sigma}_1,\boldsymbol{\sigma}_2,\ldots,\boldsymbol{\sigma}_{|I|}\rangle = \prod_{n=1}^{|I|} \hat{c}^+_{\boldsymbol{\sigma}_n}|\mathrm{vacuum}\rangle \quad (\boldsymbol{\sigma}_n \in I). \tag{5}$$

The sequence of electron creation operators in $|I\rangle$ is in ascending order, i.e., $\boldsymbol{\sigma}_i < \boldsymbol{\sigma}_j$ for $i<j$. When we add an electron to the configuration eigenstate $|I\rangle$ with the help of the electron creation operator we obtain the configuration eigenstate $|I \cup \boldsymbol{\sigma}\rangle$ up to the fermionic sign function

$$\mathrm{fsgn}(\boldsymbol{\sigma},I) = \langle I \cup \boldsymbol{\sigma}|\hat{c}^+_{\boldsymbol{\sigma}}|I\rangle. \tag{6a}$$

It gives a minus (plus) sign if it takes an odd (even) number of anticommutations to shift the operator $\hat{c}^+_{\boldsymbol{\sigma}}$ to its proper place in the sequence of electron creation operators in $|I \cup \boldsymbol{\sigma}\rangle$. In general, for $I \cap I' = \varnothing$ we define

$$\mathrm{fsgn}(I',I)\langle I \cup I'| \prod_{\substack{n=1 \\ (\boldsymbol{\sigma}_n \in I')}}^{|I'|} \hat{c}^+_{\boldsymbol{\sigma}_n}|I\rangle. \tag{6b}$$

(4) The operator which projects onto a specific configuration I is given by

$$\hat{m}_I \equiv \hat{m}_{I,I} = |I\rangle\langle I| = \prod_{\boldsymbol{\sigma}\in I} \hat{n}_{\boldsymbol{\sigma}} \prod_{\boldsymbol{\sigma}\in \overline{I}} (1-\hat{n}_{\boldsymbol{\sigma}}), \tag{7a}$$

where the operators $\hat{m}_I$ fulfill the local completeness relation

$$\sum_I \hat{m}_I = \mathbb{1}. \tag{7b}$$

At this point we also define the operators

$$\hat{n}_\varnothing = \mathbb{1}, \quad \hat{n}_I = \prod_{\boldsymbol{\sigma}\in I} \hat{n}_{\boldsymbol{\sigma}} \quad \text{for } |I| \geqslant 1, \tag{8}$$

which measure the ''gross'' occupancy of the atom. The gross occupancy operator $\hat{n}_I$ gives a nonzero result when applied to $|I'\rangle$ only if I contains electrons in the same orbitals as I'. However, I and I' need not be identical because I' could contain additional electrons in further orbitals, i.e., only $I \subseteq I'$ is required. Each gross (net) operator can be written as a sum of net (gross) operators

$$\hat{n}_I = \sum_{I' \supseteq I} \hat{m}_{I'}, \tag{9a}$$

$$\hat{m}_I = \sum_{I' \supseteq I} (-1)^{|I' \setminus I|} \hat{n}_{I'}. \tag{9b}$$

For practical calculations the net operators $\hat{m}_I$ are more useful than the gross operators $\hat{n}_I$ because the former are projection operators onto a given configuration I, i.e., $\hat{m}_I \hat{m}_{I'} = \delta_{I,I'} \hat{m}_I$, as can be seen from Eq. (7a).

(5) For $I \neq I'$ we denote $J = I \cap I'$, $I = J \cup I_1$, and $I' = J \cup I_2$ with $I_1 \cap I_2 = \varnothing$. We want to describe the transfer of $|I_1| = |I_2|$ electrons from the orbitals I_2 to the orbitals I_1, whereas the contents of the other $|J|$ orbitals remains unchanged. The gross operator for the transfer of electrons from I_2 to I_1 is given by

$$\hat{n}_{I_1,I_2} = \left(\prod_{\substack{n=1 \\ (\boldsymbol{\sigma}_n \in I_1)}}^{|I_1|} \hat{c}^+_{\boldsymbol{\sigma}_n} \right) \left(\prod_{\substack{n=1 \\ (\boldsymbol{\sigma}_n \in I_2)}}^{|I_2|} \hat{c}_{\boldsymbol{\sigma}_{|I_2|-n}} \right). \tag{10}$$

With the help of the fermionic sign function (6), the net operator for this process can be cast into the form

$$\hat{m}_{I,I'} = |I\rangle\langle I'| = \mathrm{fsgn}(J,I_1)\,\mathrm{fsgn}(J,I_2) \times \left[\prod_{\boldsymbol{\sigma}\in J} \hat{n}_{\boldsymbol{\sigma}} \prod_{\boldsymbol{\sigma}\in \overline{J \setminus (I_1 \cup I_2)}} (1-\hat{n}_{\boldsymbol{\sigma}}) \right] \hat{n}_{I_1,I_2}. \tag{11}$$

All these operators are also defined for $|I_1| \neq |I_2|$. Note the useful relation

$$\hat{m}_{I_1,I_2} \hat{m}_{I_3,I_4} = \delta_{I_2,I_3} \hat{m}_{I_1,I_4}, \tag{12}$$

which is easily proven with the help of the Dirac representation of the operators $\hat{m}_{I,I'}$.

The configuration eigenstates $|I\rangle$ form a basis of the atomic Hilbert space. The atomic Hamiltonian (2) is Hermitian, and only states with the same number of electrons are mixed. For the Hamilton matrix $(\overleftrightarrow{H}_{\rm at})_{I,I'}=\langle I|\hat{H}_{\rm at}|I'\rangle$ we can find a unitary matrix $\overleftrightarrow{T}$ such that

$$(\overleftrightarrow{T})^{+}\overleftrightarrow{H}_{\rm at}\overleftrightarrow{T}=\mathrm{diag}(E_\Gamma). \tag{13a}$$

The atomic eigenstates $|\Gamma\rangle$ obey

$$|\Gamma\rangle=\sum_I T_{I,\Gamma}|I\rangle, \tag{13b}$$

$$\hat{H}_{\rm at}|\Gamma\rangle=E_\Gamma|\Gamma\rangle, \tag{13c}$$

with

$$\sum_\Gamma T_{I,\Gamma}T^{+}_{\Gamma,I'}=\delta_{I,I'},\quad T^{+}_{\Gamma,I}\equiv T^{*}_{I,\Gamma}. \tag{13d}$$

Since only configuration eigenstates with the same number of electrons mix, the matrix $\overleftrightarrow{T}$ is block diagonal, with $|\Gamma|=|I|$ for each block.

The atomic Hamiltonian can be written as

$$\hat{H}_{\rm at}=\sum_\Gamma E_\Gamma\hat{m}_\Gamma, \tag{14a}$$

where the projection operators

$$\hat{m}_\Gamma=|\Gamma\rangle\langle\Gamma|=\sum_{I,I'}T_{I,\Gamma}\hat{m}_{I,I'}T^{+}_{\Gamma,I'} \tag{14b}$$

fulfill the local completeness relation

$$\sum_\Gamma \hat{m}_\Gamma=\mathbb{1}. \tag{14c}$$

For $\Gamma=I=\varnothing$ we set $T_{\varnothing,\varnothing}=1$. For $|\Gamma|=|I|=1$ the atomic Hamiltonian does not fix $T_{I,\Gamma}$, and we may choose them to facilitate the evaluation of expectation values for our variational wave functions.

III. GUTZWILLER-CORRELATED WAVE FUNCTIONS

A. Gutzwiller wave functions with atomic correlations

Gutzwiller-correlated wave functions are Jastrow-type wave functions, i.e., they are written as the many-particle correlator $\hat{P}_G$ acting on a normalized single-particle product state $|\Phi_0\rangle$,

$$|\Psi_G\rangle=\hat{P}_G|\Phi_0\rangle. \tag{15}$$

Expectation values with the single-particle state $|\Phi_0\rangle$ are denoted by

$$O^0\equiv\langle\hat{O}\rangle_0=\langle\Phi_0|\hat{O}|\Phi_0\rangle. \tag{16}$$

In general, these expectation values can be calculated easily with the help of Wick's theorem.[24] In the following we will assume that local Fock terms are absent in $|\Phi_0\rangle$, i.e.,

$$\langle\Phi_0|\hat{c}^{+}_{i;\boldsymbol{\sigma}}\hat{c}_{i;\boldsymbol{\sigma}'}|\Phi_0\rangle=\delta_{\boldsymbol{\sigma},\boldsymbol{\sigma}'}\langle\Phi_0|\hat{c}^{+}_{i;\boldsymbol{\sigma}}\hat{c}_{i;\boldsymbol{\sigma}}|\Phi_0\rangle=\delta_{\boldsymbol{\sigma},\boldsymbol{\sigma}'}n^0_{i;\boldsymbol{\sigma}}. \tag{17}$$

This is the case when our orbital basis is sufficiently restricted, i.e., when we use only one set of orbitals for each irreducible representation of the group of the site which we consider in $\hat{H}_1$ of Eq. (1). For cubic symmetry this means that we only consider one type of s and/or p and/or d orbitals. In cases of lower symmetry further restrictions are possible; for example, in tetragonal site symmetry s-type and $d(3z^2-r^2)$ orbitals may mix. For Hamiltonian (1), we thus choose a basis where the orbitals are not mixed locally, i.e., $t^{\boldsymbol{\sigma},\boldsymbol{\sigma}'}_{i,i}=0$ for $\boldsymbol{\sigma}\neq\boldsymbol{\sigma}'$. In the Appendix we treat the general case without these restrictions.

The one-particle state $|\Phi_0\rangle$ is usually chosen as the ground state of an effective one-particle Hamiltonian $\hat{H}^{\rm eff}_1$. Apart from the simplest cases $\hat{H}^{\rm eff}_1$ is not identical with $\hat{H}_1$; in general $\hat{H}^{\rm eff}_1$ has a lower symmetry than $\hat{H}_1$. In these cases restriction (17) may also fail.

The one-particle wave function contains many configurations which are energetically unfavorable with respect to the interacting part of the Hamiltonian. Hence the correlator $\hat{P}_G$ is chosen to suppress the weight of these configurations to minimize the total energy in Eq. (1). In the limit of strong correlations the Gutzwiller correlator $\hat{P}_G$ should project onto atomic eigenstates. Therefore, the proper multiband Gutzwiller wave function with atomic correlations reads

$$|\Psi_G\rangle=\hat{P}_G|\Phi_0\rangle=\prod_i\hat{P}_{i;G}|\Phi_0\rangle,$$

$$\hat{P}_{i;G}=\prod_\Gamma\lambda_{i;\Gamma}^{\hat{m}_{i;\Gamma}}=\prod_\Gamma[1+(\lambda_{i;\Gamma}-1)\hat{m}_{i;\Gamma}]$$

$$=1+\sum_\Gamma(\lambda_{i;\Gamma}-1)\hat{m}_{i;\Gamma}. \tag{18}$$

The 2^{2N} variational parameters $\lambda_{i;\Gamma}$ per site are real, positive numbers. For $\lambda_{i;\Gamma_0}=0$ and all other $\lambda_{i;\Gamma}\neq0$ the atomic configuration $|\Gamma_0\rangle$ at site i is removed from $|\Phi_0\rangle$.

Expectation values in Gutzwiller-correlated wave functions $|\Psi_G\rangle$ will be denoted as

$$O\equiv\langle\hat{O}\rangle=\frac{\langle\Psi_G|\hat{O}|\Psi_G\rangle}{\langle\Psi_G|\Psi_G\rangle}. \tag{19}$$

We will frequently use the expectation values for the atomic eigenstates, $m_{i;\Gamma}=\langle\hat{m}_{i;\Gamma}\rangle$, and for the gross and net occupancy operators, $n_{i;I}=\langle\hat{n}_{i,I}\rangle$ and $m_{i;I}=\langle\hat{m}_{i;I}\rangle$.

B. Exact results in infinite dimensions

Even in the one-band case the evaluation of Gutzwiller-correlated wave functions is a difficult many-particle problem; see Ref. 7 for a review. It can be solved completely in the limit of infinite dimensions without further approximations. For $d\to\infty$ the electron transfer matrix elements between two sites i and j at a distance $|i-j|=\Sigma_{l=1}{}^{d}|i_l-j_l|$ on a (hyper)cubic lattice have to be scaled as[9]

$$t_{i,j}=\overline{t}_{i,j}\left(\frac{1}{\sqrt{2d}}\right)^{|i-j|}, \tag{20}$$

where $\overline{t}_{i,j}$ is independent of the dimension. In this way the kinetic and potential energies compete with each other for all d. The bandwidth of the electrons stays finite, and we may even use the proper d-dimensional density of states $\mathcal{D}_{\boldsymbol{\sigma},0}(\epsilon)$ for our calculations. The essential simplification in the limit of infinite dimensions lies in the fact that only local properties of the wave function are needed for the calculation of single-particle properties; see Refs. 7, 25, and 26 for recent reviews on the limit of infinite dimensions.

The class of Gutzwiller-correlated wave functions as specified in Eq. (18) can also be evaluated exactly in the limit of infinite dimensions. We defer technical details of the calculations to the Appendix, and merely quote the main result of our work at this point. In the limit of infinite dimensions the expectation value of Hamiltonian (1) in terms of the Gutzwiller-correlated wave function (18) is given by

$$\langle\hat{H}\rangle=\sum_{i\neq j;\boldsymbol{\sigma}_1,\boldsymbol{\sigma}_1'}\tilde{t}_{i,j}^{\boldsymbol{\sigma}_1,\boldsymbol{\sigma}_1'}\langle\hat{c}_{i;\boldsymbol{\sigma}_1}^{+}\hat{c}_{j;\boldsymbol{\sigma}_1'}\rangle_0+\sum_{i;\boldsymbol{\sigma}}\epsilon_{i;\boldsymbol{\sigma}}n_{i;\boldsymbol{\sigma}}+\sum_{i;\Gamma}E_{i;\Gamma}m_{i;\Gamma}, \tag{21a}$$

$$\tilde{t}_{i,j}^{\boldsymbol{\sigma}_1,\boldsymbol{\sigma}_1'}=\sum_{\boldsymbol{\sigma}_2,\boldsymbol{\sigma}_2'}t_{i,j}^{\boldsymbol{\sigma}_2,\boldsymbol{\sigma}_2'}\sqrt{q_{i;\boldsymbol{\sigma}_2}^{\boldsymbol{\sigma}_1}q_{j;\boldsymbol{\sigma}_2'}^{\boldsymbol{\sigma}_1'}}. \tag{21b}$$

It is seen that the variational ground-state energy can be cast into the form of the expectation value of an effective single-particle Hamiltonian with a renormalized electron transfer matrix $\tilde{t}_{i,j}^{\boldsymbol{\sigma},\boldsymbol{\sigma}'}$. Due to the off-diagonal terms in the local interactions (2), the q factors are arranged in a nondiagonal matrix $q_{i;\boldsymbol{\sigma}}^{\boldsymbol{\sigma}'}$ which determines the quasiparticle bandwidth and the strength of band mixing in the solid state. As shown in the Appendix, the elements of the $\vec{q}$ matrix can be written as

$$\sqrt{q_{\boldsymbol{\sigma}}^{\boldsymbol{\sigma}'}}=\sqrt{\frac{1}{n_{\boldsymbol{\sigma}'}^0(1-n_{\boldsymbol{\sigma}'}^0)}}\sum_{\Gamma,\Gamma'}\sqrt{\frac{m_\Gamma m_{\Gamma'}}{m_\Gamma^0 m_{\Gamma'}^0}}\times\sum_{\substack{I,I'\\(\boldsymbol{\sigma}\notin I,\boldsymbol{\sigma}'\notin I')}}\mathrm{fsgn}(\boldsymbol{\sigma}',I')\mathrm{fsgn}(\boldsymbol{\sigma},I)\times\sqrt{m_{(I'\cup\boldsymbol{\sigma}')}^0 m_{I'}^0}T_{\Gamma,(I\cup\boldsymbol{\sigma})}^{+}T_{(I'\cup\boldsymbol{\sigma}'),\Gamma}T_{\Gamma',I'}^{+}T_{I,\Gamma'}, \tag{22}$$

where we suppressed the site index and used the definition (6) of the fermionic sign function.

Equations (21) and (22) show that we may replace the original variational parameters $\lambda_{i;\Gamma}$ by their physical counterparts, the atomic occupancies $m_{i;\Gamma}$. They are related by the simple equation

$$\lambda_{i;\Gamma}^2=\frac{m_{i;\Gamma}}{m_{i;\Gamma}^0}. \tag{23}$$

Due to the local completeness relation, the probability for an empty site is a function of the other atomic occupation densities,

$$m_{i;\varnothing}=1-\sum_{\Gamma(|\Gamma|=1)}m_{i;\Gamma}-\sum_{\Gamma(|\Gamma|\geq 2)}m_{i;\Gamma}. \tag{24}$$

For the moment we suppress the site index. As shown in the Appendix, the parameters λ_Γ^2 for atomic configurations with a single electron ($|\Gamma|=1$) are the eigenvalues of a $(2N)\times(2N)$ matrix $\vec{Z}$ whose entries are given by

$$Z_{\boldsymbol{\sigma},\boldsymbol{\sigma}'}=\frac{n_{\boldsymbol{\sigma}}^0}{m_{\boldsymbol{\sigma}}^0}\delta_{\boldsymbol{\sigma},\boldsymbol{\sigma}'}-\sum_{\Gamma(|\Gamma|\geq 2)}\frac{m_\Gamma}{m_\Gamma^0}\sum_{I(\boldsymbol{\sigma},\boldsymbol{\sigma}'\notin I)}\mathrm{fsgn}(\boldsymbol{\sigma}',I)\times\mathrm{fsgn}(\boldsymbol{\sigma},I)T_{(I\cup\boldsymbol{\sigma}'),\Gamma}T_{\Gamma,(I\cup\boldsymbol{\sigma})}^{+}\frac{m_{I\cup(\boldsymbol{\sigma},\boldsymbol{\sigma}')}^0}{m_{(\boldsymbol{\sigma},\boldsymbol{\sigma}')}^0}. \tag{25}$$

The unphysical case $m_{\boldsymbol{\sigma}}^0=0$ can safely be ignored. The matrix $\vec{Z}$ is diagonalized by a unitary matrix $\vec{T}'$,

$$(\vec{T}')^{+}\vec{Z}(\vec{T}')=\mathrm{diag}(\lambda_\Gamma^2)\quad(|\Gamma|=1), \tag{26}$$

with $T_{\boldsymbol{\sigma},\Gamma}'=T_{\boldsymbol{\sigma},\Gamma}^{*}$. These entries in the matrix $\vec{T}$ remained undetermined at the end of Sec. II.

Finally, the local densities $n_{i;\boldsymbol{\sigma}}$ can be calculated from Eq. (9a) as

$$n_{i;\boldsymbol{\sigma}}=\sum_{I(\boldsymbol{\sigma}\in I)}m_{i;I}, \tag{27a}$$

where the configuration probabilities for $|I|\geq 1$ follow from Eq. (A18b) of the Appendix,

$$m_{i;I}=\sum_K\left|\sum_\Gamma\sqrt{\frac{m_{i;\Gamma}}{m_{i;\Gamma}^0}}T_{i;\Gamma,I}^{+}T_{i;K,\Gamma}\right|^2 m_{i;K}^0. \tag{27b}$$

Hence all quantities in Eq. (21) are now expressed in terms of the variational parameters $m_{i;\Gamma}$ and the properties of $|\Phi_0\rangle$.

The remaining task is the minimization of $\langle\hat{H}\rangle$ in Eq. (21) with respect to $m_{i;\Gamma}$ and $|\Phi_0\rangle$. A conceivable though numerically unsuitable way to achieve this goal is the following. For fixed $m_{i;\Gamma}$ an input wave function $|\Phi_0^{\mathrm{in}}\rangle$ defines local occupancies $n_{i;\boldsymbol{\sigma}}^{0,\mathrm{in}}$. The wave function $|\Phi_0^{\mathrm{out}}\rangle$ is the ground state of the effective one-particle Hamiltonian

$$\hat{H}^{\mathrm{eff,\,in}}=\sum_{i\neq j;\boldsymbol{\sigma},\boldsymbol{\sigma}'}\tilde{t}_{i,j}^{\boldsymbol{\sigma},\boldsymbol{\sigma}';\mathrm{in}}\hat{c}_{i;\boldsymbol{\sigma}}^{+}\hat{c}_{j;\boldsymbol{\sigma}'}+\sum_{i;\boldsymbol{\sigma}}\tilde{\epsilon}_{i;\boldsymbol{\sigma}}^{\mathrm{in}}\hat{n}_{i;\boldsymbol{\sigma}}+\sum_{i;\Gamma}E_{i;\Gamma}m_{i;\Gamma}, \tag{28a}$$

$$\tilde{\epsilon}_{i;\boldsymbol{\sigma}}^{\mathrm{in}}=\epsilon_{i;\boldsymbol{\sigma}}\frac{n_{i;\boldsymbol{\sigma}}^{\mathrm{in}}}{n_{i;\boldsymbol{\sigma}}^{0,\mathrm{in}}}. \tag{28b}$$

Note that we have to impose the condition that the orbitals do not mix locally in our effective one-particle Hamiltonian, $\tilde{t}_{i,i}^{\boldsymbol{\sigma},\boldsymbol{\sigma}'}=\delta_{\boldsymbol{\sigma},\boldsymbol{\sigma}'}\tilde{\epsilon}_{i;\boldsymbol{\sigma}}$. The local occupancies of $|\Phi_0^{\mathrm{out}}\rangle$ serve as input for the next step in the iteration procedure. In this way the optimum $|\Phi_0^{\mathrm{opt}}\rangle$ for fixed $m_{i;\Gamma}$ is found recursively. After

the global minimization of $\langle \hat{H} \rangle$ with respect to the parameters $m_{i;\Gamma}$ the optimum effective one-particle Hamiltonian $\hat{H}^{\text{eff, opt}}$ defines a quasiparticle band structure which is suitable for a comparison with experiments. Furthermore, it can be used to derive the low-temperature thermodynamics. Naturally, the application of $\hat{H}^{\text{eff, opt}}$ is restricted to the description of the low-energy physics (Fermi-liquid regime).[7,12,13]

Another route to finite temperatures is the following. The variational ground-state energy is a function of the occupancies in momentum space. Hence it can be used to derive Fermi-liquid parameters[27] which give access to the low-energy physics of metallic correlated-electron systems.[28,29]

C. Gutzwiller wave functions with pure density correlations

If we ignore the nondiagonal terms $\mathcal{J}_i^{\sigma_1,\sigma_2;\sigma_3,\sigma_4}$ in the atomic Hamiltonian (2), we may set

$$T_{I,\Gamma} \equiv \delta_{I,\Gamma} \tag{29}$$

in all the formulas of Sec. III B. Under these conditions we recover the Gutzwiller wave functions with pure density correlations. In fact, for this class of Gutzwiller wave functions the variational ground-state energy is independent of the nondiagonal terms $\mathcal{J}_i^{\sigma_1,\sigma_2;\sigma_3,\sigma_4}$. This is ultimately due to the fact that the correlator does not change the orbital occupation, and that Fock terms vanish in $|\Phi_0\rangle$ according to Eq. (17).

Under condition (29), the $\overleftrightarrow{Z}$ matrix in Eq. (25) is diagonal. We use the fact that

$$n_{i;\sigma} = m_{i;\sigma} + \sum_{I(|I|\geq 2, \sigma \in I)} m_{i;I} \tag{30}$$

due to Eq. (9) so that the eigenvalues of $\overleftrightarrow{Z}$ can be written as

$$\lambda_{i;\sigma}^2 = \frac{n_{i;\sigma}^0 - n_{i;\sigma} + m_{i;\sigma}}{m_{i;\sigma}^0}. \tag{31}$$

Hence, for consistency with Eq. (23), we should have

$$n_{i;\sigma} = n_{i;\sigma}^0 \tag{32}$$

for Gutzwiller-correlated wave functions with pure density correlations. This result can be derived more directly. As shown in the Appendix, in infinite dimensions we have

$$\langle \hat{n}_{i;\sigma} \rangle = \langle \hat{P}_{i;\mathrm{G}} \hat{n}_{i;\sigma} \hat{P}_{i;\mathrm{G}} \rangle_0 = \langle \hat{n}_{i;\sigma} \hat{P}_{i;\mathrm{G}}^2 \rangle_0 . \tag{33}$$

For the second step we used the fact that now the Gutzwiller correlator contains density operators only; compare Eq. (18). With the help of Eq. (A12b), result (32) follows immediately. Thus Eqs. (30) and (32) allow us to express explicitly the probabilities for a single occupancy in terms of the local densities in $|\Phi_0\rangle$ and the variational parameters $m_{i;I}$ for $|I| \geq 2$.

For pure density correlations and for wave functions which obey Eq. (17), different local configurations are not mixed. Consequently, the $\overleftrightarrow{q}$ matrix becomes diagonal, as can be shown explicitly from Eq. (22) with the help of Eq. (29). For the diagonal elements we find

$$\sqrt{q_{i;\sigma}} \equiv \sqrt{q_{i;\sigma}^{\sigma}} = \sqrt{\frac{1}{n_{i;\sigma}^0 (1 - n_{i;\sigma}^0)}} \sum_{I(\sigma \notin I)} \sqrt{m_{i;I} m_{i;(I \cup \sigma)}}, \tag{34a}$$

and the expectation value of the Hamiltonian reduces to

$$\langle \hat{H} \rangle = \sum_{i \neq j;\sigma,\sigma'} t_{i,j}^{\sigma,\sigma'} \sqrt{q_{i;\sigma}} \sqrt{q_{j;\sigma'}} \langle \hat{c}_{i;\sigma}^{+} \hat{c}_{j;\sigma'} \rangle_0 + \sum_{i;\sigma} \epsilon_{i;\sigma} n_{i;\sigma}^0 + \sum_{i;I} U_{i;I} m_{i;I}, \tag{34b}$$

where

$$U_{i;I} = \langle I | \hat{H}_{i;\mathrm{at}} | I \rangle = \sum_{\sigma,\sigma' \in I} \mathcal{U}_i^{\sigma,\sigma'} . \tag{34c}$$

For translationally invariant systems the above equations (34) were first derived in Refs. 17 and 18 using a generalized Gutzwiller approximation scheme. A concise description of this semiclassical counting approach can be found in Ref. 27; for a mathematically well-defined procedure, see Ref. 30. The wave function used in Refs. 17, 18, and 20 was defined as

$$|\Psi_{\mathrm{G}}\rangle = \hat{P}_G' |\Psi_0\rangle$$

$$\hat{P}_G' = \prod_i \prod_{I(|I| \geq 2)} g_{i;I}^{\hat{m}_{i;I}} . \tag{35}$$

The wave functions $|\Psi_0\rangle$ and $|\Phi_0\rangle$ are related by the transformation[31]

$$|\Psi_0\rangle = \hat{P}_{\mathrm{SP}} |\Phi_0\rangle, \tag{36a}$$

$$\hat{P}_{\mathrm{SP}} = \prod_i g_{i;\varnothing} \prod_{\sigma=1}^{2N} g_{i;\sigma}^{\hat{n}_{i;\sigma}} . \tag{36b}$$

Since $\hat{P}_{\mathrm{SP}}$ contains single-particle operators only, both $|\Psi_0\rangle$ and $|\Phi_0\rangle$ are single-particle wave functions. The relation between the parameters $g_{i;I}$ and $\lambda_{i;I}$ is given by

$$g_{i;\varnothing} = \lambda_{i;\varnothing}, \tag{37a}$$

$$g_{i;\sigma} = \frac{\lambda_{i;\sigma}}{\lambda_{i;\varnothing}}, \tag{37b}$$

$$g_{i;I} = \frac{\lambda_{i;I} \lambda_{i;\varnothing}^{|I|-1}}{\Pi_{\sigma \in I} \lambda_{i;\sigma}} \quad (|I| \geq 2), \tag{37c}$$

and

$$g_{i;I}^2 = \frac{m_{i;\varnothing}^{|I|-1} m_{i;I}}{\Pi_{\sigma \in I} m_{i;\sigma}} \quad (|I| \geq 2) \tag{37d}$$

holds in infinite dimensions.

Independently, expressions (34) were derived by Hasegawa[32] and Frésard and Kotliar,[33] who used a generalization of the Kotliar-Ruckenstein slave-boson mean-field approach[11] introduced by Dorin and Schlottmann.[34] In Ref. 20 we proved that the results of these approximate treatments are variationally controlled in the limit of infinite dimen-

TABLE I. Eigenstates with symmetry specifications, spin quantum numbers, energies, and notation symbols for the 16 $N=2$ atomic configurations.

No.	Atomic eigenstate $\|\Gamma\rangle$	Symmetry	$S_{\rm at}$	$S^z_{\rm at}$	energy E_Γ	prob.
1	$\|0,0\rangle$	a_1	0	0	0	e
2	$\|\uparrow,0\rangle$	e_g	1/2	1/2	0	$s_\uparrow$
3	$\|0,\uparrow\rangle$	e_g	1/2	1/2	0	$s_\uparrow$
4	$\|\downarrow,0\rangle$	e_g	1/2	$-1/2$	0	$s_\downarrow$
5	$\|0,\downarrow\rangle$	e_g	1/2	$-1/2$	0	$s_\downarrow$
6	$\|\uparrow,\uparrow\rangle$	${}^3A_2$	1	1	$U'-J$	$d_t^{\uparrow\uparrow}$
7	$(\|\uparrow,\downarrow\rangle+\|\downarrow,\uparrow\rangle)/\sqrt{2}$	${}^3A_2$	1	0	$U'-J$	d_t^{0}
8	$\|\downarrow,\downarrow\rangle$	${}^3A_2$	1	-1	$U'-J$	$d_t^{\downarrow\downarrow}$
9	$(\|\uparrow,\downarrow\rangle-\|\downarrow,\uparrow\rangle)/\sqrt{2}$	${}^1E$	0	0	$U'+J$	d_E
10	$(\|\uparrow\downarrow,0\rangle-\|0,\uparrow\downarrow\rangle)/\sqrt{2}$	${}^1E$	0	0	$U-J_{\rm C}$	d_E
11	$(\|\uparrow\downarrow,0\rangle+\|0,\uparrow\downarrow\rangle)/\sqrt{2}$	${}^1A_1$	0	0	$U+J_{\rm C}$	d_A
12	$\|\uparrow,\uparrow\downarrow\rangle$	E_g	1/2	1/2	$U+2U'-J$	$t_\uparrow$
13	$\|\uparrow\downarrow,\uparrow\rangle$	E_g	1/2	1/2	$U+2U'-J$	$t_\uparrow$
14	$\|\downarrow,\uparrow\downarrow\rangle$	E_g	1/2	$-1/2$	$U+2U'-J$	$t_\downarrow$
15	$\|\uparrow\downarrow,\downarrow\rangle$	E_g	1/2	$-1/2$	$U+2U'-J$	$t_\downarrow$
16	$\|\uparrow\downarrow,\uparrow\downarrow\rangle$	A_1	0	0	$2U+4U'-2J$	f

sions; see Ref. 20 for further comparison with previous variational and slave-boson mean-field approaches to degenerate-band systems.

IV. TWO DEGENERATE BANDS

The formulas derived in the Appendix are completely general, and apply for all atomic Hamiltonians (2) and for all kinds of symmetry breaking in the one-particle wave function $|\Phi_0\rangle$. Depending on the complexity of the problem, the numerical treatment of multiband correlations may become rather involved. It appears to be a good strategy to study the two-band case first, which provides the simplest example of a correlated multiband model. To keep our expressions for the $\vec{q}$ and $\vec{Z}$ matrices as simple as possible, we chose a simple cubic lattice with one atomic site per cell and two degenerate $d(e_g)$ orbitals per atom. This model should reflect the situation of nickel to some extent. For example, Ni^{2+}, e.g. in NiO, exhibits two $d(e_g)$ holes in a high-spin state, and metallic nickel has approximately one d hole per site.

Alternatively, we could have chosen atoms with two $p_{(x,y)}$ orbitals on a square lattice. However, such a model might be less meaningful for the study of ferromagnetic transitions since, as we will see below, these strongly depend on the structure of the density of states, which depends sensitively on the dimension. In addition, our formulas become exact for Gutzwiller-correlated wave functions in the limit of infinite dimensions, and $1/d$ corrections are expected to be much smaller in three than in two dimensions. From our experience in the one-band case[10,12,35] we conjecture that the differences between $d=3$ and $d=\infty$ are actually marginal.

A. Atomic Hamiltonian

We label the orbitals $d(3z^2-r^2)$ as $b=1$ and $d(x^2-y^2)$ as $b=2$, and introduce the spin index $\sigma=\uparrow,\downarrow$. There are four spin orbitals per atom, leading to $2^4=16$ multielectron configurations (see Table I). Then the atomic Hamiltonian reads

$$\hat{H}_{\rm at}=U\sum_b \hat{n}_{b,\uparrow}\hat{n}_{b,\downarrow}+U'\sum_{\sigma,\sigma'}\hat{n}_{1,\sigma}\hat{n}_{2,\sigma'}-J\sum_\sigma \hat{n}_{1,\sigma}\hat{n}_{2,\sigma}$$
$$+J\sum_\sigma \hat{c}^+_{1,\sigma}\hat{c}^+_{2,-\sigma}\hat{c}_{1,-\sigma}\hat{c}_{2,\sigma}+J_{\rm C}(\hat{c}^+_{1,\uparrow}\hat{c}^+_{1,\downarrow}\hat{c}_{2,\downarrow}\hat{c}_{2,\uparrow}$$
$$+\hat{c}^+_{2,\uparrow}\hat{c}^+_{2,\downarrow}\hat{c}_{1,\downarrow}\hat{c}_{1,\uparrow}). \tag{38}$$

For two orbitals, $\hat{H}_{\rm at}$ exhausts all possible two-body interaction terms.

All 16 eigenstates and their respective energies are given in Table I. The one-electron states and, due to the particle-hole symmetry, all three-electron states are seen to be degenerate. The only nontrivial cases are the two-electron states. The model of two degenerate $d(e_g)$ orbitals leads to the following restrictions enforced by symmetry: first, as we can use real wave functions for $d(e_g)$ orbitals, the relation $J=J_C$ holds; second, the relation $U-U'=2J$ follows from the cubic symmetry.[23] To see this we address the six two-electron states. There is one spin triplet ${}^3A_2$ with the energy $U'-J$. In addition, there are three spin singlets: one, with symmetry ${}^1A_1$, has the energy $U+J_C$, whereas the other two have the energies $U'+J$ and $U-J_C$, respectively. Cubic symmetry requires[23] that these two form the degenerate doublet ${}^1E$. This symmetry requirement can be derived by a transformation into the equivalent basis $|3y^2-r^2\rangle$ and $|z^2-x^2\rangle$.

For Gutzwiller wave functions with pure density correlations, exchange-type interactions [the second line in Eq. (38)] do not contribute to the variational ground-state energy. If we ignore these terms in Eq. (38), all configurations $|I\rangle$ are eigenstates of the resulting $\hat{H}^{\rm dens}_{\rm at}$. In addition to the states with zero, one, three, and four electrons as listed in Table I,

TABLE II. Two-electron spin-orbit states with spin quantum numbers, energies, and notation symbols for the case of pure density correlations.

No.	Wave function $\|I\rangle$	$S^z_{\rm at}$	energy U_I	prob.
6	$\|\uparrow,\uparrow\rangle$	1	$U'-J$	$d_1^{\uparrow\uparrow}$
7	$\|\downarrow,\downarrow\rangle$	-1	$U'-J$	$d_1^{\downarrow\downarrow}$
8	$\|\downarrow,\uparrow\rangle$	0	U'	d_s
9	$\|\uparrow,\downarrow\rangle$	0	U'	d_s
10	$\|\uparrow\downarrow,0\rangle$	0	U	d_c
11	$\|0,\uparrow\downarrow\rangle$	0	U	d_c

the energies of the two-electron states are grouped into three doublets. As listed in Table II, there are (i) two components of the spin triplet with $|S_z|=1$ at the energy $U'-J$, (ii) states $|\uparrow,\downarrow\rangle$ and $|\downarrow,\uparrow\rangle$ at energy U', and (iii) states $|0,\uparrow\downarrow\rangle$ and $|\uparrow\downarrow,0\rangle$ at energy U.

B. One-particle Hamiltonian and density of states

We will use an orthogonal tight-binding Hamiltonian with first- and second-nearest-neighbor hopping matrix elements. Furthermore, we apply the two-center approximation for the hopping matrix elements, and exclude any spin-flip hopping. Then the matrix elements in momentum space between the $3z^2-r^2$ $(b=1)$ and the x^2-y^2 $(b=2)$ orbitals are given by[36]

$$\begin{aligned}\epsilon_1(k)=&\,t^{(1)}_{dd\sigma}(\tfrac{1}{2}\cos k_x+\tfrac{1}{2}\cos k_y+2\cos k_z)\\&+\tfrac{3}{2}\,t^{(1)}_{dd\delta}(\cos k_x+\cos k_y)+t^{(2)}_{dd\sigma}\cos k_x\cos k_y\\&+[\tfrac{1}{4}\,t^{(2)}_{dd\sigma}+3t^{(2)}_{dd\pi}](\cos k_x+\cos k_y)\cos k_z\\&+3t^{(2)}_{dd\delta}(\cos k_x\cos k_y+\tfrac{1}{4}\cos k_x\cos k_z+\tfrac{1}{4}\cos k_y\cos k_z),\end{aligned}\tag{39a}$$

$$\begin{aligned}\epsilon_2(k)=&\,\tfrac{3}{2}\,t^{(1)}_{dd\sigma}(\cos k_x+\cos k_y)\\&+t^{(1)}_{dd\delta}(\tfrac{1}{2}\cos k_x+\tfrac{1}{2}\cos k_y+2\cos k_z)\\&+4t^{(2)}_{dd\pi}\cos k_x\cos k_y\\&+[\tfrac{3}{4}\,t^{(2)}_{dd\sigma}+t^{(2)}_{dd\pi}+\tfrac{9}{4}\,t^{(2)}_{dd\delta}](\cos k_x+\cos k_y)\cos k_z,\end{aligned}\tag{39b}$$

and the band mixing is given by

$$\begin{aligned}\epsilon_{12}(k)=\epsilon_{21}(k)=&\,(\sqrt{3}/2)[-t^{(1)}_{dd\sigma}+t^{(1)}_{dd\delta}](\cos k_x-\cos k_y)\\&+[(\sqrt{3}/4)t^{(2)}_{dd\sigma}-\sqrt{3}t^{(2)}_{dd\pi}+(3\sqrt{3}/4)t^{(2)}_{dd\delta}]\\&\times(\cos k_x-\cos k_y)\cos k_z.\end{aligned}\tag{39c}$$

Here we set the cubic lattice constant equal to unity. As in Refs. 17 and 18 the hopping parameters were chosen according to general experience for transition-metal energy bands, $t^{(1)}_{dd\sigma}=1$ eV, $t^{(2)}_{dd\sigma}=0.25$ eV and $t^{(1),(2)}_{dd\sigma}:t^{(1),(2)}_{dd\pi}:t^{(1),(2)}_{dd\delta}=1:(-0.3):0.1$. This choice avoids pathological features in the energy bands such as perfect nesting at half-filling.

The one-particle part of Hamiltonian (1) is easily diagonalized in momentum space via the transformations

$$\eta^+_{k;1,\sigma}=\cos\phi_k\hat{c}^+_{k;1,\sigma}+\sin\phi_k\hat{c}^+_{k;2,\sigma},\tag{40a}$$

$$\eta^+_{k;2,\sigma}=-\sin\phi_k\hat{c}^+_{k;1,\sigma}+\cos\phi_k\hat{c}^+_{k;2,\sigma},\tag{40b}$$

with

$$\tan(2\phi_k)=\frac{2\epsilon_{12}(k)}{\epsilon_1(k)-\epsilon_2(k)}.\tag{40c}$$

The dispersion relations for the η bands become

$$E_{1,2}(k)=\frac{\epsilon_1(k)+\epsilon_2(k)}{2}\pm\sqrt{\left(\frac{\epsilon_1(k)-\epsilon_2(k)}{2}\right)^2+[\epsilon_{12}(k)]^2}.\tag{41}$$

The η bands are degenerate along the line (ξ,ξ,ξ) in the irreducible Brillouin zone, and the total bandwidth is $W=6.6$ eV. Our one-particle state $|\Phi_0\rangle$ is chosen as

$$|\Phi_0\rangle=\prod_\sigma\prod_{(E_{1,2}(k)\le E_{F,\sigma})}\hat{\eta}^+_{k;1,\sigma}\hat{\eta}^+_{k;2,\sigma}|\text{vacuum}\rangle.\tag{42}$$

The Fermi surfaces of both η bands are invariant under the symmetry operations of the lattice.

Condition (17) is fulfilled due to the degeneracy of the e_g orbitals. For the same reason the projected orbital densities of states

$$\begin{aligned}\mathcal{D}_1(\epsilon)=&\,\frac{1}{L}\sum_k\cos^2(\phi_k)\,\delta[\epsilon-E_1(k)]\\&+\sin^2(\phi_k)\,\delta[\epsilon-E_2(k)],\\\mathcal{D}_2(\epsilon)=&\,\frac{1}{L}\sum_k\sin^2(\phi_k)\,\delta[\epsilon-E_1(k)]\\&+\cos^2(\phi_k)\,\delta[\epsilon-E_2(k)],\end{aligned}\tag{43}$$

have to be identical, $\mathcal{D}_1(\epsilon)=\mathcal{D}_2(\epsilon)\equiv\mathcal{D}_0(\epsilon)/2$, and

$$n^0_{b,\sigma}=\tfrac{1}{2}\int_{-\infty}^{E_{F,\sigma}}d\epsilon\;\mathcal{D}_0(\epsilon)\tag{44}$$

is independent of the band index, $n^0_{1,\sigma}=n^0_{2,\sigma}\equiv n^0_\sigma$.

Since we built in the cubic symmetry into our starting wave function $|\Phi_0\rangle$ and our atomic Hamiltonian (38) preserves this symmetry, our self-consistency cycle will not change this property. Therefore, we may set $s_{1,\sigma}=s_{2,\sigma}\equiv s_\sigma$ and $t_{1,\sigma}=t_{2,\sigma}\equiv t_\sigma$ for our variational parameters; compare Table I for the notation. Note that the number of $\uparrow$ electrons and $\downarrow$ electrons need not be the same; i.e., we still allow for band ferromagnetism.

For the study of the ferromagnetic transition it is helpful to consider the density of states at the Fermi energy, $\mathcal{D}_0(E_{F,\sigma})$. This quantity as a function of the band-filling fraction n_σ is displayed in Fig. 1. Later, we will study the half-filled case, $n_\sigma=0.5$, in the context of the Brinkman-Rice metal-to-insulator transition, and the fillings $n_\sigma=0.29$ and 0.35 for ferromagnetism. The case $n_\sigma=0.29$ corresponds to a

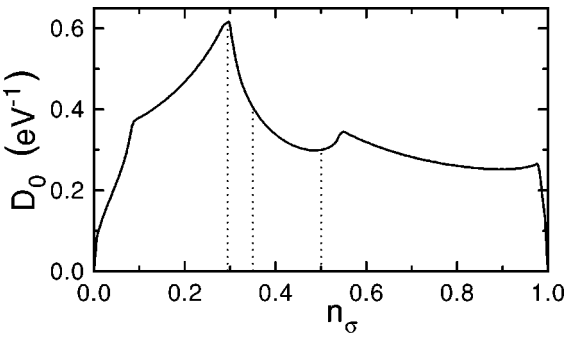

FIG. 1. Model density of states at the Fermi energy as a function of the band filling $n_{\boldsymbol{\sigma}}=n/4$. The dashed lines indicate the fillings used in Sec. IV. The total bandwidth is $W=6.6$ eV.

maximum in the density of states at the Fermi energy. There we expect the strongest tendency to ferromagnetism.

In this work we take the viewpoint of the canonical rather than the grand-canonical ensemble. This means that we keep the zero of energy fixed for all band fillings. Then the Fermi energy moves as a function of the band filling, and is different for the two spin species in the case of ferromagnetism. Of course, this does not change the results because we could have kept the Fermi energy the same for both bands and shifted the minority band against the majority band to vary the magnetization density.

C. Variational ground-state energy

Now we derive the explicit form of the ground-state energy functional (21) for our example. To this end we first show that the matrix $\overleftrightarrow{Z}$ in Eq. (25) is diagonal. From Table I we see that for $|\Gamma|>2$ the atomic eigenstates are also configuration eigenstates, $T_{I,\Gamma}=\delta_{I,\Gamma}$. In this case, the factors $T_{(J\cup\boldsymbol{\sigma}),\Gamma}T^{+}_{\Gamma,(J\cup\boldsymbol{\sigma}')}$ require $J\cup\boldsymbol{\sigma}=I=J\cup\boldsymbol{\sigma}'$, i.e., $\boldsymbol{\sigma}=\boldsymbol{\sigma}'$. For $|\Gamma|=2$ we note that $J=\boldsymbol{\gamma}$ with $\boldsymbol{\gamma}\neq\boldsymbol{\sigma},\boldsymbol{\sigma}'$ has to hold. Now that $|\Gamma\rangle=\sqrt{1/2}[|\boldsymbol{\sigma}_1,\boldsymbol{\sigma}_2\rangle\pm|\boldsymbol{\sigma}_3,\boldsymbol{\sigma}_4\rangle]$ according to Table I, we see again that $\boldsymbol{\sigma}=\boldsymbol{\sigma}'$ must hold since either $(\boldsymbol{\gamma},\boldsymbol{\sigma})=(\boldsymbol{\sigma}_1,\boldsymbol{\sigma}_2)=(\boldsymbol{\gamma},\boldsymbol{\sigma}')$ or $(\boldsymbol{\gamma},\boldsymbol{\sigma})=(\boldsymbol{\sigma}_3,\boldsymbol{\sigma}_4)=(\boldsymbol{\gamma},\boldsymbol{\sigma}')$ must be fulfilled $[(\boldsymbol{\sigma}_1,\boldsymbol{\sigma}_2)\cap(\boldsymbol{\sigma}_3,\boldsymbol{\sigma}_4)=\varnothing]$. Since the $\overleftrightarrow{Z}$ matrix is diagonal it follows that the matrix $T'_{\boldsymbol{\sigma},\Gamma}$ is the unit matrix.

The eigenvalues of the $\overleftrightarrow{Z}$ matrix are $\lambda^2_{\boldsymbol{\sigma}}=m_{\boldsymbol{\sigma}}/m^0_{\boldsymbol{\sigma}}$. Then the relation

$$m^0_\Gamma=m^0_I \tag{45}$$

is fulfilled for all Γ, I with $|\Gamma|=|I|$. We then find from Eq. (24) that

$$s_\sigma=n^0_\sigma-[d^{\sigma\sigma}_t+t_{-\sigma}+2t_\sigma+f+\tfrac{1}{2}(d_A+2d_E+d^0_t)] \tag{46a}$$

gives the probabilities for a single occupancy in terms of the multiple occupancies which serve as our variational parameters; see Table I for the notation. The probability for an empty site follows from the completeness relation (14c) as

$$e=1-2n^0_\uparrow-2n^0_\downarrow+d^{\uparrow\uparrow}_t+d^{\downarrow\downarrow}_t+d^0_t+d_A+2d_E+4t_\uparrow+4t_\downarrow+3f. \tag{46b}$$

Along the same lines it can be shown that Eq. (27b) reduces to

$$m_I=\sum_\Gamma |T_{I,\Gamma}|^2 m_\Gamma . \tag{47a}$$

With the help of Eqs. (25) and (45), it then follows that

$$n_\sigma=n^0_\sigma \tag{47b}$$

holds in our model. Similar arguments to those used to show that the $\overleftrightarrow{Z}$ matrix is diagonal can be employed to show that the matrix $\overleftrightarrow{q}$ is diagonal. Furthermore, the degeneracy of the orbitals due to the cubic symmetry requires

$$q^{\boldsymbol{\sigma}}_{\boldsymbol{\sigma}}\equiv q_\sigma . \tag{47c}$$

Hence the dispersion relations of the η bands are rescaled by the same factor q such that $|\Phi_0\rangle$ is unchanged, and our self-consistency cycle terminates after a single iteration. Thus the optimum $|\Phi_0\rangle$ can be chosen from the start. Nevertheless, we still allow for ferromagnetism, since $E_{F,\sigma}$ remained undetermined thus far.

A straightforward calculation gives the explicit form of the q factors,

$$q_\sigma=\frac{1}{n^0_\sigma(1-n^0_\sigma)}[(\sqrt{t_\sigma}+\sqrt{s_{-\sigma}})^{\frac{1}{2}}(\sqrt{d_A}+2\sqrt{d_E}+\sqrt{d^0_t}) +\sqrt{s_\sigma}(\sqrt{e}+\sqrt{d^{\sigma\sigma}_t})+\sqrt{t_{-\sigma}}(\sqrt{d^{(-\sigma)(-\sigma)}_t}+\sqrt{f})]^2. \tag{48}$$

We denote the kinetic energy of the $(1,\sigma)$ and $(2,\sigma)$ electrons in the uncorrelated state $|\Phi_0\rangle$ by

$$\overline{\epsilon}_{\sigma,0}=\int_{-\infty}^{E_{F,\sigma}} d\epsilon\ \epsilon\mathcal{D}_0(\epsilon). \tag{49}$$

With the help of Table I, we may then cast the minimization problem into the form

$$E^{\text{var, atom}}=\sum_\sigma q_\sigma\overline{\epsilon}_{\sigma,0}+(U'-J)(d^{\uparrow\uparrow}_t+d^{\downarrow\downarrow}_t+d^0_t) +2(U'+J)d_E+(U+J)d_A +(2U+4U'-2J)(t_\uparrow+t_\downarrow+f). \tag{50}$$

This expression must be minimized with respect to the eight variational parameters, $d^{\uparrow\uparrow}_t$, $d^{\downarrow\downarrow}_t$, d^0_t, d^0_t, d_E, d_A, $t_\uparrow$, $t_\downarrow$, and f for a given band filling n_σ. In a paramagnetic situation, $n_\uparrow=n_\downarrow$, the number of variational parameters is reduced to five by the relations $d^{\sigma\sigma}_t=d^0_t\equiv d_t$, $t_\sigma\equiv t$, and $q_\sigma=q$. Furthermore, the relations $s_\uparrow=s_\downarrow$ and $\overline{\epsilon}_{\downarrow,0}=\overline{\epsilon}_{\uparrow,0}$ hold.

For Gutzwiller wave functions with density correlations we employ Eqs. (34) and the notations of Table II. Now the variational problem reads

$$E^{\text{var, dens}}=\sum_\sigma \tilde{q}_\sigma\overline{\epsilon}_{\sigma,0}+(U'-J)(d^{\uparrow\uparrow}_1+d^{\downarrow\downarrow}_1)+2U'd_s+2Ud_c +(2U+4U'-2J)(t_\uparrow+t_\downarrow+f). \tag{51a}$$

Here the q factors are given by

$$\tilde{q}_\sigma=\frac{1}{n_\sigma^0(1-n_\sigma^0)}[(\sqrt{t_\sigma}+\sqrt{s_{-\sigma}})(\sqrt{d_c}+\sqrt{d_s}) + \sqrt{s_\sigma}(\sqrt{e}+\sqrt{d_1^{\sigma\sigma}})+\sqrt{t_{-\sigma}}(\sqrt{d_1^{(-\sigma)(-\sigma)}}+\sqrt{f})]^2. \tag{51b}$$

In this case our variational parameters are $d_1^{\uparrow\uparrow}$, $d_1^{\downarrow\downarrow}$, d_s, d_c, $t_\uparrow$, $t_\downarrow$, and f. The probabilities for an empty site e and a singly occupied site s_σ are related to the variational parameters by

$$s_\sigma=n_\sigma^0-[d_1^{\sigma\sigma}+t_{-\sigma}+2t_\sigma+f+d_c+d_s], \tag{52a}$$

$$e=1-2n_\uparrow^0-2n_\downarrow^0+d_1^{\uparrow\uparrow}+d_1^{\downarrow\downarrow}+2d_s+2d_c+4t_\uparrow+4t_\downarrow+3f. \tag{52b}$$

Expression (51) is identical to the one used in Refs. 17, 18, and 32.

D. Brinkman-Rice metal-insulator transition at half-band-filling

As a first application of our variational treatment we study the Brinkman-Rice metal-to-insulator transition. For a single band and a translationally invariant system we recover the original Gutzwiller wave function.[3] In infinite dimensions this wave function at half-band-filling is known to describe a continuous transition from the paramagnetic metal to a paramagnetic insulator at $U=U_{\mathrm{BR}}$ above which all electrons are localized (Brinkman-Rice insulator).[5] It can be shown, though, that the Brinkman-Rice transition at a finite interaction strength is the consequence of the large-d limit, i.e., it is not contained in the wave function for any finite dimension.[37] Hence statements on the metal-insulator transition based on our variational description must be taken with care. Even in infinite dimensions the Brinkman-Rice transition can be concealed by an (antiferromagnetically) ordered phase; see Ref. 38 for the one-band case, and Ref. 32 for $N=2$. It should be clear, though, that the onset of long-range order crucially depends on the choice of the matrix elements for the electron transfer. In general, there is no perfect nesting between the Fermi surface and the Brillouin zone, such that antiferromagnetism is not expected to set in for small interaction strengths.

For multiband systems the Brinkman-Rice transition occurs at integer numbers $1\leqslant n\leqslant 2N-1$ of electrons per atom. For two bands the transitions for $n=1$ or 3 are continuous as in the one-band case. There, our results do not differ much from those given in Ref. 17 for Gutzwiller wave functions with pure density correlations. Thus we focus on the case $n=2$, where, in general, the transition is *discontinuous* in the bandwidth reduction factor q. This means that a jump occurs at the Brinkman-Rice transition from the finite value q_{BR} in the metallic phase to $q=0$ in the insulating phase.

For $n=2$ the dependence of the five variational parameters d_t, d_E, d_A, t, and f as a function of the interaction strength U is shown in Fig. 2. Here, the value $J=0.2U$ ($U'=0.6U$) was chosen. For $U=0$ (independent electrons) the values of all quantities are equal. As U becomes larger the spin-triplet double occupancy d_t increasingly dominates the other multiple occupancies; in particular, this is true close to the jump at U_{BR}. All multiple occupancies are discontinuous at the Brinkman-Rice transition, since, in the insulating case, all electrons are frozen into local spin triplets, i.e., we have $d_t=\frac{1}{3}$ and all other multiple occupancies are zero. Note that in the case of pure density correlations the dominance of d_t is less pronounced; compare Fig. 2 of Ref. 17.

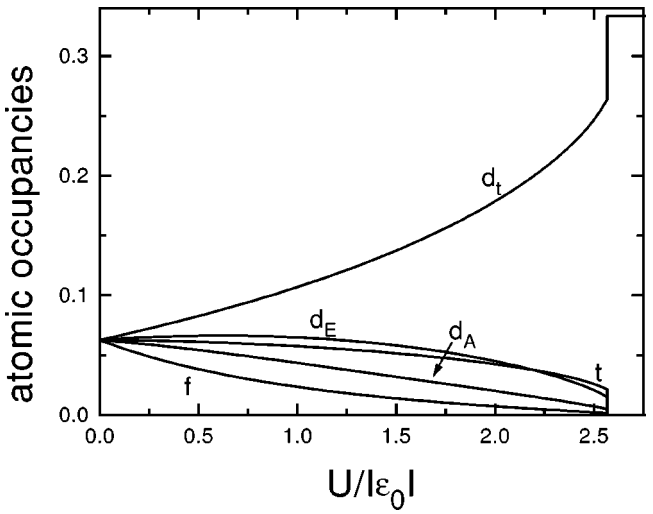

FIG. 2. Variational parameters as a function of U for $J=0.2U$ ($U'=0.6U$) at half-band-filling.

In Fig. 3 the q values are shown as a function of U for various J/U ratios. The singular case $J=0$ ($U=U'$) differs from the generic situation both qualitatively and quantitatively. The Brinkman-Rice transition is continuous *only* at this point, and values of J/U as small as 10^{-2} produce finite jumps of a significant size. A (realistic) value of $U'=0.8U$ ($J=0.1U$) is enough to reduce the critical interaction strength U_{BR} for the Brinkman-Rice transition by a factor of 2; see Fig. 3. Only for $U'=U$ ($J=0$) all atomic two-electron states are degenerate in energy. Thus, near the Brinkman-Rice transition, all double occupancies have equal weight, both in the metallic and insulating phases. Any finite J value will remove the degeneracies and reestablish the generic case. At the singular point of zero configuration width,[4] the critical interaction strength can be given by an analytical expression, first derived by Lu.[39]

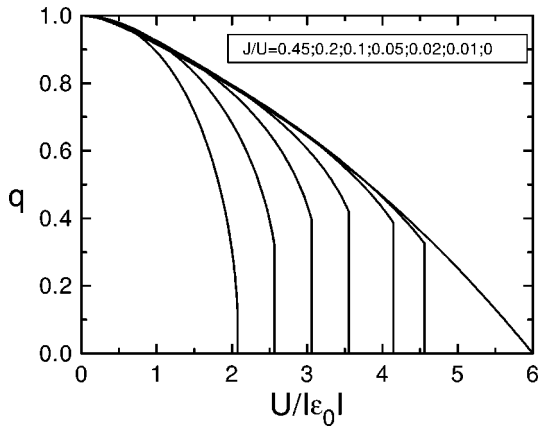

FIG. 3. Bandwidth renormalization factor q at half-band-filling as a function of U for various values of J [$J=(U-U')/2$].

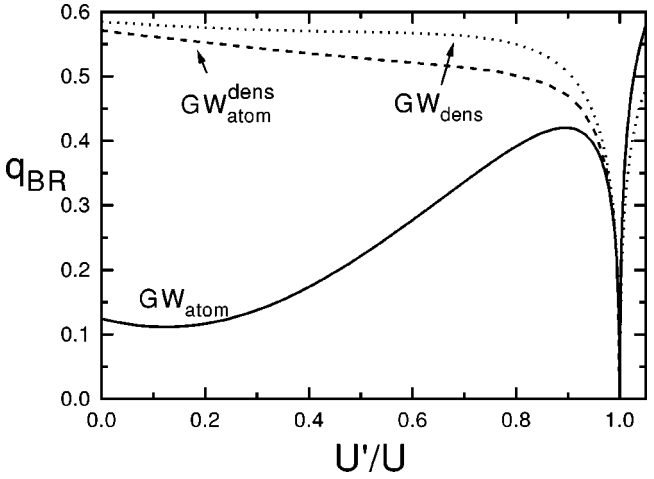

FIG. 4. Bandwidth renormalization factor at the Brinkman-Rice transition $U=U_{BR}$ as a function of U'/U for the Gutzwiller wave function with atomic correlations (full line) and pure density correlations (dotted line). Also shown is the value of the q factor for GW_{atom} at $U=U_{BR}^{dens}$ (dashed line).

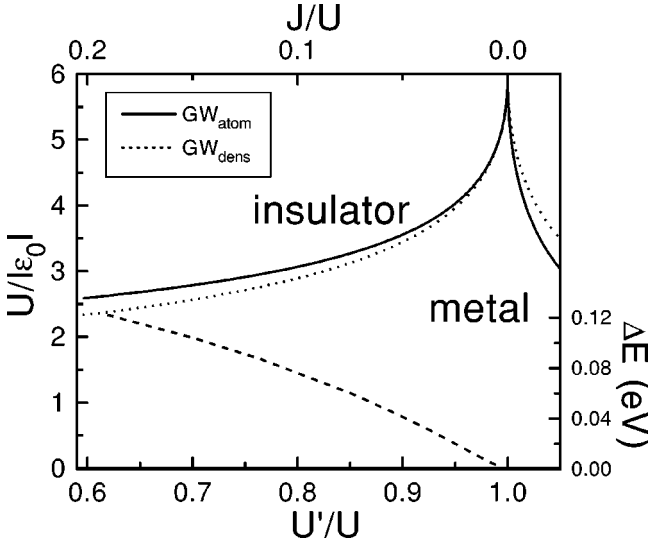

FIG. 5. Phase diagram and critical interaction strength for the Brinkman-Rice transition in Gutzwiller wave functions with atomic (GW_{atom}) and pure density (GW_{dens}) correlations as a function of U'/U (left Y axis). The dashed curve shows the energy gain for atomic correlations against pure density correlations at $U=U_{BR}^{dens}$ (right Y axis).

As seen from Fig. 3 the critical interaction strength U_{BR} and the size of the q factor strongly depend on the size of the Hund's-rule coupling J/U. In Fig. 4 we display the behavior of q_{BR} as a function of U'/U at the corresponding critical interaction strengths U_{BR}. For the Gutzwiller wave function with atomic correlations (GW_{atom}) a maximum of $q_{BR}^{max} \approx 0.4$ for $U'<U$ occurs near $U'/U=0.9$ ($J/U=0.05$). A shallow minimum of $q_{BR}^{min} \approx 0.1$ is seen near $U'/U \approx 0.14$ ($J/U=0.43$). Conversely, the same curve for the Gutzwiller wave function with pure density correlations (GW_{dens}) increases monotonically as a function of J/U toward $q_{BR}^{dens} \approx 0.6$ at $U'/U=0$.

In the range $0 \leqslant U'/U<1$, we always find $q_{BR}^{dens} > q_{BR}$. Moreover, we have $U_{BR} > U_{BR}^{dens}$ (see Fig. 5). As expected, the metallic state is stabilized by the introduction of the full atomic correlations. Nevertheless, the two values for the Brinkman-Rice transition are fairly close to each other, $U_{BR} \gtrsim U_{BR}^{dens}$. Therefore, it is interesting to plot the value of the q factor for the case of atomic correlations at $U=U_{BR}^{dens}$. This is very similar to the q_{BR} curve for pure density correlations (see Fig. 4). It shows that the q factor sharply—yet continuously—drops as a function of U in the region $U_{BR}^{dens} \leqslant U<U_{BR}$ before it jumps from q_{BR} to zero at the Brinkman-Rice transition.

The Brinkman-Rice transition is discontinuous because the ''metallic'' and ''insulating'' minima compete for the global minimum of the variational energy function. In contrast to the one-parameter minimization problem of the single-band case (and the two-band case for $J=0$) the metallic minimum does not smoothly develop into the insulating one in the presence of more than one atomic energy scale. The size of the q-factor jump measures the difference between the variational parameters in the metallic and insulating phases. Small discontinuities imply that the variational parameters of the metallic state at the transition are close to those of the Brinkman-Rice insulator. For large q_{BR} the metallic and insulating minima are well separated in parameter space.

In the Brinkman-Rice insulator all sites are in the state with lowest atomic energy. In the metal higher atomic states are mixed in. The strength of the mixing depends on the energy separation between the atomic levels. For example, the three $S=1$ configurations at energy $U-3J$ are separated from the singlet ^1E at energy $U-J$ by $2J$. Therefore, the $S=1$ configurations dominate the metallic state near the Brinkman-Rice transition for large J, and q_{BR} decreases with increasing J. When J becomes too large, near $U'=0$ ($J/U=0.5$), the energy of the three-electron states $3U-5J$ is approaching the energies of the two-electron states. Thus the value of t is enhanced at the expense of the d_t parameter. Consequently, q_{BR} increases again. In the case of pure density correlations, the two $|S_z|=0$ configurations $|\uparrow,\uparrow\rangle$ and $|\downarrow,\downarrow\rangle$ have energies $U-3J$ not too much lower than the two configurations $|\uparrow,\downarrow\rangle$ and $|\downarrow,\uparrow\rangle$, with energies $U-2J$. This leads to a competition of the respective occupancies for all J, and q_{BR}^{dens} is a fairly smooth function of J.

In Fig. 5 we display the paramagnetic (U,U') phase diagram at half-band-filling. It is seen that the additional atomic correlations (GW_{atom}) stabilize the metallic phase for all $U>U'$ ($J>0$) compared to the result of the density correlations. The figure also shows the gain in the variational energy when we use the Gutzwiller wave functions with full atomic correlations instead of pure density correlations. The gain is shown for fixed value $U=U_{BR}^{dens}$ as a function of U'/U. It is quite considerable, of the order of 0.1 eV, for realistic values of $J/U \approx 0.1$.

For $J<0$ ($U'>U$), the metal is *less* stable in the presence of full atomic correlations. Note that in this parameter range the insulating ground state is different for the two variational wave functions: a unique atomic $^1A_1$ state with energy $U-|J|$ versus two degenerate $|\uparrow\downarrow,0\rangle$ and $|0,\uparrow\downarrow\rangle$ states of energy U for pure density correlations. As a consequence, in this limit the violation of the atomic symmetry leads to a qualitatively different result for pure density correlations.

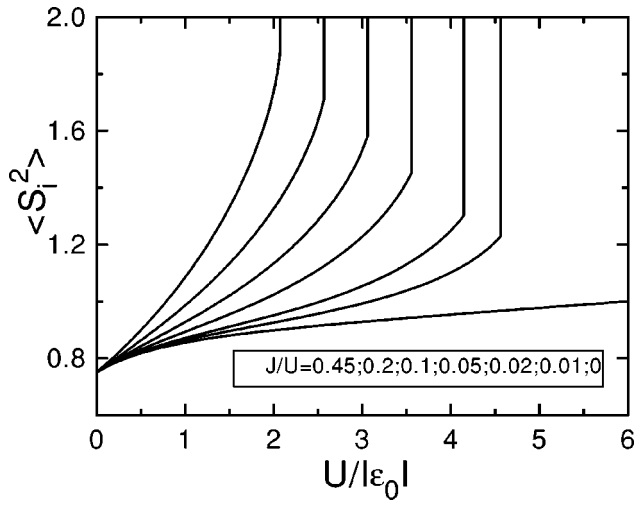

FIG. 6. Size of the local spin $\langle(\hat{\vec{S}}_i)^2\rangle$ in the paramagnetic Gutzwiller wave function with atomic correlations as a function of the interaction strength and various values of $J=(U-U')/2$ for half-band-filling.

Finally, in Fig. 6, we display the size of the local spin $\langle(\vec{S}_i)^2\rangle = S_i(S_i+1)$ at half-band-filling. In the Brinkman-Rice insulator we have $S_i(S_i+1)=2$ ($S_i=1$) when $J>0$. For $J<0$ the local spin drops to zero at U_{BR}, since the singlet $^1A_1$ is the local ground-state configuration in the Brinkman-Rice insulator. We again focus on $J\geqslant 0$. For non-interacting electrons ($U=0$) simple statistical arguments apply, and the local spin is readily found to be $(1/2)(1+1/2)(8/16)+1(1+1)(3/16)=\frac{3}{4}$.

For $J=0$ the local spin increases very slowly with U, up to $1(1+1)(3/6)=1$ at U_{BR} and above. Recall that for $J=0$ the Brinkman-Rice insulator is highly degenerate. For $J>0$ the weight of the local triplets becomes more and more important toward the Brinkman-Rice transition. This leads to local spin values for $U=U_{\mathrm{BR}}$ as large as $S_i(S_i+1)=1.55$ for $J/U=0.1$, and even $S_i(S_i+1)=1.8$ for $J/U=0.45$. As seen above in Fig. 4, the increase in the local spin is most prominent close to the Brinkman-Rice transition, which again demonstrates the drastic change in the multiple occupancies there.

E. Itinerant ferromagnetism

The formulas we derived in Sec. IV C apply equally for the case of ferromagnetism. In this subsection we allow for a finite magnetization density M per band in the z direction,

$$0\leqslant M=(n_{b,\uparrow}-n_{b,\downarrow})/2\leqslant M_{\mathrm{sat}}=n/4. \tag{53}$$

In Fig. 7, the magnetization M is shown as a function of U for fixed $J/U=0.2$ ($U'/U=0.6$). The critical interaction for the ferromagnetic transition, U_F^{atom}, is about a factor 2 larger than its value U_F^{HF} obtained from the Hartree-Fock-Stoner theory. The corresponding values U_F^{dens} always lie somewhat below the values for the Gutzwiller wave function with atomic correlations. In general, the relation $M_{\mathrm{HF}}(U)>M_{\mathrm{dens}}(U)>M_{\mathrm{atom}}(U)$ holds, i.e., for all interaction strengths the tendency to ferromagnetism is strongest within the Hartree-Fock theory and weakest for Gutzwiller wave functions with atomic correlations. Furthermore, the slopes of $M(U)$ are much steeper in the Hartree-Fock results than in the presence of correlations.

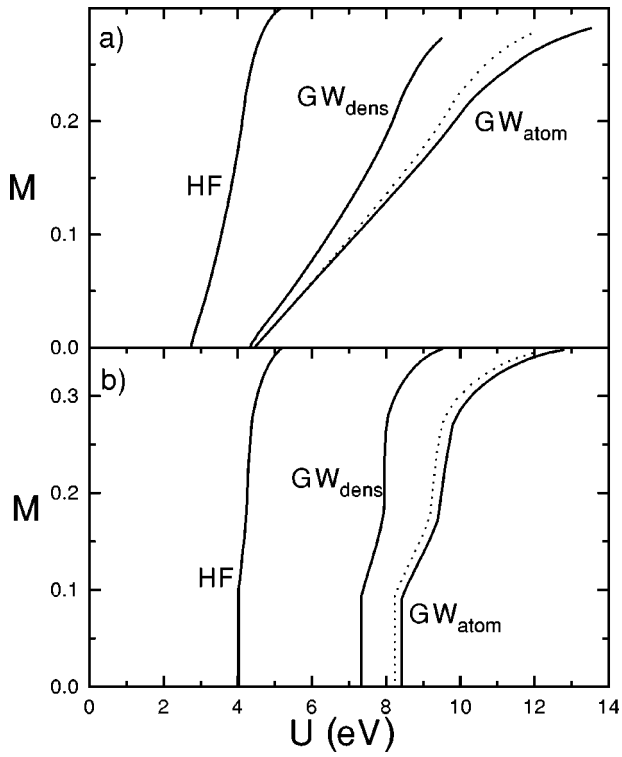

FIG. 7. Magnetization density per band as a function of U for $J=0.2U$ for the Hartree-Fock (HF) solution, the Gutzwiller wave function with pure density correlations (GW_{dens}), and the Gutzwiller wave function with atomic correlations (GW_{atom}) for (a) $n/4=0.29$ and (b) $n/4=0.35$. The dotted line indicates the results for GW_{atom} with $J_C=0$.

The properties of the ferromagnetic phase strongly depend on the spectrum of the atomic two-electron configurations. To further analyze this point, we included the case of $J_C=0$, which changes only the excited two-electron states. A shift of the curve $M(U)$ results toward smaller interaction strengths; for a given magnetization density a smaller interaction strength is required as compared to the correct symmetry case $J=J_C$ (see Fig. 7). The effect is more pronounced when we go to the Gutzwiller wave function with pure density correlations. In this case all exchange terms in Eq. (38) are neglected. Then, even the ground state is modified since the atomic spin triplet with $S^z=0$ moves up in energy into the range of the atomic spin singlets. Again, the magnetization curve shifts to (much) smaller interaction strengths. Both results indicate how strongly itinerant ferromagnetism is influenced by the atomic n-electron spectra.

In Fig. 7(a) we chose the particle density per band to be $n/4=0.29$ (more precisely, $n/4=0.2941$), right at the maximum of the density of state curve; compare Fig. 1. For this case there are finite slopes of the $M(U)$ curves at U_F, and a ''Stoner criterion'' for the onset of ferromagnetism applies. In Fig. 7(b) we chose the particle density per band as $n/4=0.35$. As seen from the density of states in Fig. 1, the density of states at the Fermi energy $\mathcal{D}_0(E_{F,\uparrow})+\mathcal{D}_0(E_{F,\downarrow})$ first *increases* as a function of the magnetization density,

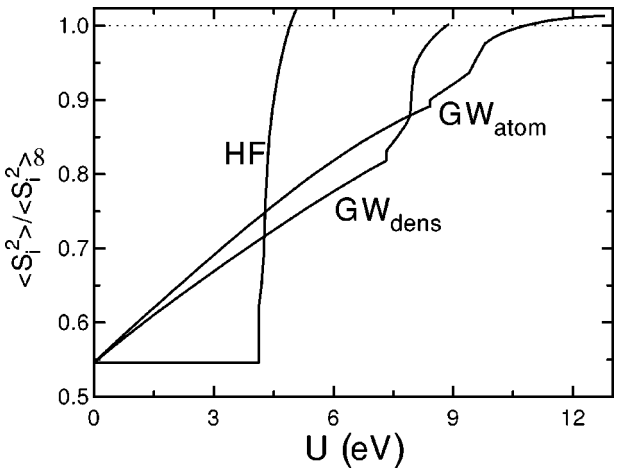

FIG. 8. Size of the local spin $\langle(\hat{\vec{S}}_i)^2\rangle$ as a function of the interaction strength for $J=0.2U$ and band filling $n/4=0.35$ for the Hartree-Fock (HF) theory and the Gutzwiller wave functions ($GW_{\rm dens}$, $GW_{\rm atom}$).

and, therefore, a discontinuous transition occurs from the paramagnet to the ferromagnet.

In the case of pure density correlations a second jump in the $M(U)$ curve is observed, which is absent in the other two curves. As discussed in Ref. 18, this jump is related to another feature of the density of states. In the Hartree-Fock theory this feature is too weak to be of any significance in comparison to the interaction energy. When the full atomic correlations are taken into account, this first-order jump at a finite magnetization density disappears due to the enhanced flexibility of the variational wave function. Nevertheless, in this range of a strongly varying magnetization density we find rapid variations of the various double occupancies, quite similar to the behavior near the Brinkman-Rice transition for $n/4=0.5$.

Another remarkable difference between the Hartree-Fock and Gutzwiller methods lies in the approach to ferromagnetic saturation. In the Hartree-Fock theory the magnetization saturates at U values about 20–40 % above the onset of ferromagnetism at $U_F^{\rm HF}$. In contrast, in the variational approach saturation is reached at about twice the onset value, $U_{\rm sat} \lesssim 2U_F$. However, even when the minority-spin occupancies are zero and $\langle\hat{S}_z^{\rm at}\rangle$ is constant, the majority-spin occupancies $s_\uparrow$ and $d_t^{\uparrow\uparrow}$ vary with U, since the limit of zero empty sites is reached only for $U\to\infty$.

The magnitude of the local spin as a function of U is shown in Fig. 8. For $U\to\infty$ each site is either singly occupied with probability $2-n$ or doubly occupied (spin $S=1$) with probability $n-1$. Hence $\langle(\vec{S}_i)^2\rangle_\infty=\frac{3}{4}(2-n)+2(n-1)=5(n/4)-\frac{1}{2}$. For the correlated wave functions this limit is reached from *above* since, for $U<\infty$, charge fluctuations first increase the number of spin-1 sites at the expense of spin-$\frac{1}{2}$ sites, which turn into empty sites. A further decrease of U will also activate the singlet double occupancies and higher multiple occupancies. Thus the local spin eventually reduces below $\langle(\vec{S}_i)^2\rangle_\infty$. Conversely, Hartree-Fock theory does not give the proper large-U limit for the local spin. Instead, the Hartree-Fock limit is given by $\langle(\vec{S}_i)^2\rangle_\infty^{\rm HF}=(n/4)(3+n/2)$.

The change of $\langle(\vec{S}_i)^2\rangle$ at U_F is only a minor effect within the correlated-electron approach. In particular, this holds for the case of atomic correlations, where about 90% of the local spin saturation value is already reached in the paramagnetic state. Again, the Hartree-Fock results are completely different. There the local spin sharply increases as a function of the interaction strength, since the absence of correlations fixes $\langle(\vec{S}_i)^2\rangle^{\rm HF}(U<U_F^{\rm HF})=\langle(\vec{S}_i)^2\rangle(U=0)$.

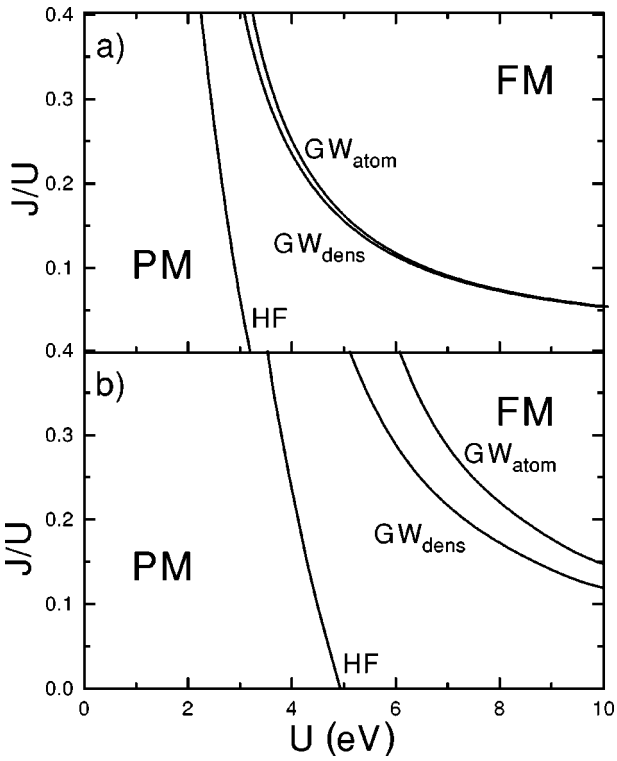

FIG. 9. Phase diagram as a function of U and J for the Hartree-Fock (HF) solution and the two Gutzwiller wave functions ($GW_{\rm dens}$, $GW_{\rm atom}$) for (a) $n/4=0.29$ and (b) $n/4=0.35$; PM: paramagnet, FM: ferromagnet.

In Fig. 9 we display the J/U phase diagram for both fillings. It shows that Hartree-Fock theory always predicts a ferromagnetic instability. In contrast, the correlated-electron approach strongly supports the idea that a substantial on-site exchange is required for the occurrence of ferromagnetism at realistic interaction strengths. For the case $n/4=0.29$, the differences between the phase diagrams for the two correlated-electron wave functions are minor. Due to the large density of states at the Fermi energy, the critical interaction strengths for the ferromagnetic transition are comparably small, and the densities for the double occupancies in both correlated wave functions do not differ much. For the larger band filling $n/4=0.35$, i.e., away from the peak in the density of state, the values for U_F are larger, and, in the atomic correlation case, the Gutzwiller wave functions can more easily generate local spin triplets while keeping the global paramagnetic phase.

Finally, in Fig. 10, we display the energy differences between the paramagnetic and ferromagnetic ground states as a function of the interaction strength for $J=0.1U$. For the correlated-electron case this quantity is of the order of the Curie temperature which is in the range of 100–1000 K in real materials. On the other hand, the Hartree-Fock theory yields small condensation energies only in the range of U

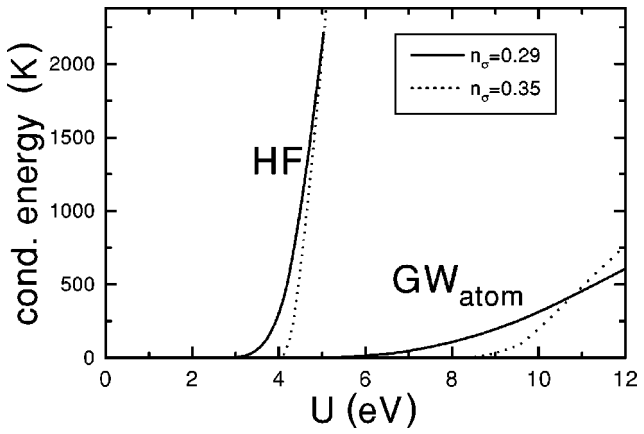

FIG. 10. Condensation energy as a function of U for $J=0.2U$ for the Hartree-Fock (HF) theory and the Gutzwiller wave function (GW_{atom}) for $n_\sigma=n/4=0.29$ (full lines) and $n_\sigma=n/4=0.35$ (dashed lines).

$\approx$4 eV; for larger U, the condensation energy is of order U. Including the correlation effects we have relatively small condensation energies even for interaction values as large as twice the bandwidth ($U\approx 10$ eV).

V. SUMMARY AND CONCLUSIONS

In this work we constructed Gutzwiller-correlated wave functions with atomic correlations for general multiband Hubbard models. We evaluated these many-particle wave functions in the limit of infinite space dimensions ($d=\infty$) for the general atomic Hamiltonian for all interaction strengths without any restrictions on the electron transfer matrix elements between orbitals on the same or on different lattice sites. Within the metallic phase the differences between three and infinite dimensions were found to be small for the Gutzwiller wave function for a single band.[10,12,35] Therefore, we expect that our results are very applicable for the case of physical interest.

Our variational states consist of a Jastrow-type many-particle correlator which acts on an appropriate Hartree-Fock single-particle product wave function. The Gutzwiller correlator is chosen to modify the occurrence of atomic multielectron eigenstates $|\Gamma_i\rangle$ as compared to the uncorrelated (statistical) case. Therefore, our trial states are exact both in the noninteracting and atomic limits, and they incorporate the essential competition between local and itinerant features of interacting multiband systems.

The atomic single-particle states of appropriate symmetry (spin orbits) constitute the basis for our one-electron Hamiltonian which describes the motion of the electrons through the solid, and provides the Hartree-Fock wave function. The atomic multielectron configurations $|I_i\rangle$ are product states (Slater determinants) made from the spin-orbit states. If the (on-site) electron-electron interaction contains only density-type two-particle interactions, the configurations $|I_i\rangle$ will not couple, and the local probabilities $m_{i;I}$ of these $\mathfrak{n}$-electron configurations ($\mathfrak{n}=|I|$) can be used as variational parameters to minimize the ground-state energy. In general, however, the states $|I_i\rangle$ do not exhibit the correct symmetry of atomic $\mathfrak{n}$-electron eigenstates $|\Gamma_i\rangle$. The correct symmetry can be established only when all exchange-type terms of the atomic Hamiltonian are taken into account, i.e., all atomic correlations must be included from the beginning. Hence all configurations $|I_i\rangle$ within the subspace $|I_i|=\mathfrak{n}$ are coupled, and the diagonalization of the atomic Hamiltonian by unitary matrices $T_{i;I,\Gamma}$ results in the $\mathfrak{n}$-electron atomic eigenstates $|\Gamma_i\rangle$. Therefore, the multiple occupancies $m_{i;\Gamma}$ for the atomic eigenstates are the appropriate variational parameters in our problem. In many cases the elements of the matrices $\overleftrightarrow{T}$ are given by symmetry alone; in general, however, they must be obtained from the diagonalization of the atomic Hamiltonian.

The exact results in infinite dimensions can be cast into the form of an *effective* single-particle Hamiltonian with reduced electron transfers between the lattice sites. Since the atomic eigenstates are nontrivial linear combinations of one-particle (spin-orbit) product states, the hopping reduction factors are arranged in a $2N\times 2N$ matrix $q_{\boldsymbol{\sigma}}^{\boldsymbol{\sigma}'}$ with spin-orbit indices $\boldsymbol{\sigma}$ and $\boldsymbol{\sigma}'$. These quantities are nontrivial functions of (i) the variational parameters $m_{i;\Gamma}$, (ii) the local occupancies of the Hartree-Fock wave function, and (iii) the one-electron densities in the interacting case. The derivation of the latter requires the diagonalization of a $2N\times 2N$ matrix $\overleftrightarrow{Z}$. Further complexities occur for the most general case, i.e., for an extended spin-orbit basis with more than one orbital type per representation of the symmetry group of the atomic site. Here we have nonzero values for the orbital-nondiagonal parts of the on-site one-particle expectation values. At the expense of another unitary transformation this most general case is also covered by our formalism. Naturally, this leads to a more complicated structure for the matrices $\overleftrightarrow{q}$ and $\overleftrightarrow{Z}$ and the effective local hybridizations and one-particle densities.

Like the density-functional theory, the variational method is intrinsically limited to the description of ground-state properties, e.g., the ground-state energy, compressibility, magnetization, and magnetic susceptibility. Similar to the density-functional theory our variational approach naturally extends to finite temperatures and low-frequency excitations, since our variational ground-state energy corresponds to that of an effective one-particle Hamiltonian. The ''correlated bands'' of this Hamiltonian can be used for a comparison with measured dispersion curves and effective masses. Note that our approach is completely general, and applies to all multiband systems. Therefore, we hope that it will be fruitful for a description of correlated electron systems in the metallic phase. Naturally, any quasiparticle approach is limited to the region of the validity of Fermi-liquid theory.

In this work we presented explicit results for a degenerate two-band model as the simplest nontrivial application of our method. We assumed e_g-type orbitals on sites of a simple cubic lattice. For the single-particle Hamiltonian, nearest- and next-nearest neighbor transfer matrix elements were used which give rise to two bands of width $W=6.6$ eV. In our model we included all possible two-particle interactions. Yet, there exist only two independent interaction parameters U and J, since the relation $U-U'=2J$ holds due to symmetry, and, likewise, $J_C=J$ is fulfilled for the charge exchange term. For our simple model system the $\overleftrightarrow{Z}$ matrix is the unit matrix and the hopping reduction matrix is diagonal.

As a first application we studied the Brinkman-Rice metal-insulator transition at half-band-filling. Above some

finite interaction strength all electrons localize. As for the one-band case this localization transition is rather questionable as a scenario for the Mott transition in multiband Mott-Hubbard systems. The lattice sites will not be isolated as in the Brinkman-Rice insulator but they will remain coupled via the itinerant exchange. Thus, in the large-U limit, we should expect an antiferromagnetic insulating ground state for $J>0$ whereas, for $J<0$, antiferro-type orbital ordering appears to be most likely.

Apart from the singular point $J=0$ the metal-insulator transition is discontinuous, as manifests itself in finite changes q_{BR} of the bandwidth reduction factor at the transition. The results for Gutzwiller wave functions with atomic correlations significantly differ from those for pure density correlations. In particular, this applies to the behavior of the curves $q_{\mathrm{BR}}(J/U_{\mathrm{BR}})$ for large J, which monotonously increases (decreases) as a function of J for atomic (pure density) correlations for $J/U>0.05$. The Gutzwiller wave function with atomic correlations is seen to be more ''flexible'' than that with pure density correlations in the sense that the metallic state can much better adapt itself to the (Brinkman-Rice) insulator.

The general aspect of a discontinuous metal-insulator transition could be generic for multiband Hubbard models. In the insulator the atoms are dominantly in a specific $\mathfrak{n}$-electron ground state which is compatible with Hund's first rule. Other $\mathfrak{n}$-electron states (of excitation energy J), even more $\mathfrak{n}\pm1$ electron states (excitation energies U), are separated from the ground state by finite gaps. In the metallic phase a macroscopic number of energetically unfavorable $\mathfrak{n}\pm1$ electron states is created and, consequently, also a macroscopic number of the other $\mathfrak{n}$-electron states. It does not seem to be very likely that all of these occupation densities change continuously at a *single* critical interaction strength. Instead, the metallic state breaks down discontinuously when the gain in kinetic energy can no longer compensate the intraatomic gaps. However, variational statements on the nature of the transition between the metal and the Mott-Hubbard insulator must be taken with great care.[6,7]

Nonetheless, we expect, for reasonably small J/U and for the case of a general band structure without the perfect-nesting property, that there will exist a transition to an antiferromagnetic state with strong electronic localization, i.e., with large charge-transfer excitation energies. We do not expect transitions to an antiferromagnetic metallic or small-gap insulating state. Yet to test this conjecture an antiferromagnetic trial state needs to be investigated.

As a second application we addressed the issue of itinerant ferromagnetism. For this purpose we chose two band fillings, the first one at the maximum of the density of states, the second one close to it. Again, we found a large ''flexibility'' of the Gutzwiller wave function with atomic correlations: the paramagnetic state accommodates large local spins, as much as 90% of the saturation value, and only a small jump is observed at the ferromagnetic transition. Hence the paramagnetic metallic state near the transition and, moreover, the ferromagnetic state are highly correlated.

In general, the ferromagnetic transition is found to occur at fairly large interaction strengths U_F, with values $1<U_F/W\lesssim2$. In addition, finite values of the exchange interaction J are required with $J_{\mathrm{min}}\approx0.1U$. These results may change toward smaller values of (J,U) if a larger value for the peak density of states is chosen. In any case, our results stress the importance of the atomic Hund's-rule exchange for ferromagnetism in multiband models, a view fostered a long time ago by van Vleck.[1] The ferromagnetic condensation energy is an estimate for k_BT_C, the Curie temperature for iron-group metals. It is found to be of right order of magnitude, $T_C\approx500$ K, for interaction strengths as large as 10 eV. The condensation energy is a smooth function of the interaction strength, i.e., the ground-state magnetization does not too sensitively depend on U.

In contrast, the corresponding Hartree-Fock treatment yields completely different results. The ferromagnetic transition is predicted to occur for small values of U, with $U_F^{\mathrm{HF}}/W<1$. The magnitude of the spin exchange J is relatively unimportant, and the magnetization saturates almost immediately as a function of U. Finally, apart from a small interval above U_F^{HF}, the condensation energy is grossly overestimated. Thus itinerant ferromagnetism in interacting multiband systems is a correlated-electron problem that cannot be treated within a weak-coupling approach.

The inferior results of the Hartree-Fock treatment might be taken as an indication that spin-density-functional theory is also inadequate for the description of itinerant ferromagnetism in iron-group metals because our results suggest strong correlation effects there. On the other hand, the success of this effective single-particle theory may point to an inadequacy of our multiband model for the following reason. The results from spin-density-functional theory indicate that the minority-spin bands are broader and, accordingly, the corresponding wave functions more extended in space than those of the majority bands. This ''orbital flexibility'' makes the minority-spin density to dominate in the interstitial regions. Orbital flexibility is not included in the present form of our multiband models. If considered, e.g., by extending the orbital basis, the required interaction strength for ferromagnetism may be reduced considerably toward a less correlated situation. In principle, our treatment of generalized Gutzwiller wave functions allows us to incorporate such basis extensions. Work in this direction is in progress, and applications of our general formalism to real systems are presently under investigation.

ACKNOWLEDGMENT

J.B. thanks P. Nozières for an invitation to the ILL, where this project was started.

APPENDIX: EVALUATION OF EXPECTATION VALUES

In this appendix we sketch the essential steps for the exact evaluation of Gutzwiller-correlated wave functions in infinite dimensions. First, we choose a basis in which local Fock terms are absent. Second, we select appropriate expansion parameters for a perturbation theory around the limit of zero interactions. As a third step we set up a diagrammatic theory for the calculation of expectation values based on Wick's theorem and the linked-cluster theorem.[24] The clue to an exact solution in infinite dimensions is the selection of the expansion parameters. They are chosen in such a way that all higher-order diagrams vanish in infinite dimensions, and the

trivial order gives the exact result. Further technical details can be found in Refs. 12, 13, and 20. In the rest of the Appendix we derive explicit results for the local multiple occupancies and the interacting one-particle density matrix.

1. Change of the local basis

For a general $|\Phi_0\rangle$ the noninteracting local one-particle matrix $\overleftrightarrow{C}_i^0$ with the entries

$$C^0_{i;\boldsymbol{\gamma},\boldsymbol{\gamma}'}=\langle\Phi_0|\hat{c}^+_{i;\boldsymbol{\gamma}}\hat{c}_{i;\boldsymbol{\gamma}'}|\Phi_0\rangle \tag{A1}$$

is not diagonal. Therefore, we derive the formalism here which covers the most general case.

Since our diagrammatic approach for the evaluation of Gutzwiller-correlated wave functions requires that local Fock terms are absent, we need to perform a local unitary transformation,

$$\sum_{\boldsymbol{\gamma}} F^+_{i;\boldsymbol{\sigma},\boldsymbol{\gamma}}F_{i;\boldsymbol{\gamma},\boldsymbol{\sigma}'}=\delta_{\boldsymbol{\sigma},\boldsymbol{\sigma}'}, \tag{A2a}$$

$$\hat{h}^+_{i;\boldsymbol{\sigma}}=\sum_{\boldsymbol{\gamma}} F^+_{i;\boldsymbol{\sigma},\boldsymbol{\gamma}}\hat{c}^+_{i;\boldsymbol{\gamma}},\quad \hat{c}^+_{i;\boldsymbol{\gamma}}=\sum_{\boldsymbol{\sigma}} F_{i;\boldsymbol{\gamma},\boldsymbol{\sigma}}\hat{h}^+_{i;\boldsymbol{\sigma}}, \tag{A2b}$$

$$\hat{h}_{i;\boldsymbol{\sigma}}=\sum_{\boldsymbol{\gamma}} F_{i;\boldsymbol{\gamma},\boldsymbol{\sigma}}\hat{c}_{i;\boldsymbol{\gamma}},\quad \hat{c}_{i;\boldsymbol{\gamma}}=\sum_{\boldsymbol{\sigma}} F^+_{i;\boldsymbol{\sigma},\boldsymbol{\gamma}}\hat{h}_{i;\boldsymbol{\sigma}}. \tag{A2c}$$

This diagonalizes the noninteracting local one-particle density matrix

$$(\overleftrightarrow{F}_i)^+\overleftrightarrow{C}^0_i\overleftrightarrow{F}_i=\mathrm{diag}(n^{h,0}_{i;\boldsymbol{\sigma}}). \tag{A3a}$$

This is always possible because $\overleftrightarrow{C}_i^0$ is Hermitian. As seen from Eq. (A3a), local Fock terms are absent in the new basis, i.e., the noninteracting local one-particle density matrix $\overleftrightarrow{H}_i^0$ is diagonal,

$$\begin{aligned}H^0_{i;\boldsymbol{\sigma},\boldsymbol{\sigma}'}&=\langle\Phi_0|\hat{h}^+_{i;\boldsymbol{\sigma}}\hat{h}_{i;\boldsymbol{\sigma}'}|\Phi_0\rangle=\delta_{\boldsymbol{\sigma},\boldsymbol{\sigma}'}\langle\Phi_0|\hat{h}^+_{i;\boldsymbol{\sigma}}\hat{h}_{i;\boldsymbol{\sigma}}|\Phi_0\rangle\\&=\delta_{\boldsymbol{\sigma},\boldsymbol{\sigma}'}n^{h,0}_{i;\boldsymbol{\sigma}}.\end{aligned} \tag{A3b}$$

For a given $|\Phi_0\rangle$ the transformation matrix $\overleftrightarrow{F}_i$ is fixed, and the local occupancies $n^{h,0}_{i;\boldsymbol{\sigma}}$ in the new basis are the eigenvalues of $\overleftrightarrow{C}_i^0$.

From now on we work in the new local basis. We suppress the site index for the rest of this subsection. The notation of Sec. II B remains essentially the same but each operator $\hat{c}^+_{\boldsymbol{\sigma}}$ ($\hat{c}_{\boldsymbol{\sigma}}$) has to be replaced by $\hat{h}^+_{\boldsymbol{\sigma}}$ ($\hat{h}_{\boldsymbol{\sigma}}$). In the new basis the configuration eigenstates are denoted by

$$|\mathcal{H}\rangle=\prod_{n=1}^{|\mathcal{H}|}\hat{h}^+_{\boldsymbol{\sigma}_n}|\mathrm{vacuum}\rangle\quad(\boldsymbol{\sigma}_n\in\mathcal{H}), \tag{A4a}$$

and the atomic eigenstates $|\Gamma\rangle$ and their projection operator $m_\Gamma=|\Gamma\rangle\langle\Gamma|$ are given by

$$|\Gamma\rangle=\sum_{\mathcal{H}} A_{\mathcal{H},\Gamma}|\mathcal{H}\rangle, \tag{A4b}$$

$$\hat{m}_\Gamma=\sum_{\mathcal{H},\mathcal{H}'} A_{\mathcal{H},\Gamma}\hat{m}_{\mathcal{H},\mathcal{H}'}A^+_{\Gamma,\mathcal{H}'}. \tag{A4c}$$

The elements of the unitary matrix $\overleftrightarrow{A}$ are given by

$$A_{\mathcal{H},\Gamma}=\langle\mathcal{H}|\Gamma\rangle=\sum_I T_{I,\Gamma}\langle\mathcal{H}|I\rangle,$$

$$\langle\mathcal{H}|I\rangle=\det(F_{\boldsymbol{\gamma}_i,\boldsymbol{\sigma}_j}),\quad(\boldsymbol{\gamma}_i\in I,\boldsymbol{\sigma}_j\in\mathcal{H}). \tag{A5a}$$

The inverse relation to Eq. (A5a) reads

$$T_{I,\Gamma}=\sum_{\mathcal{H}} A_{\mathcal{H},\Gamma}\langle I|\mathcal{H}\rangle. \tag{A5b}$$

Again, $\overleftrightarrow{A}$ is block-diagonal. Equations (A5) are defined for $|\Gamma|=|\mathcal{H}|\geqslant 2$. For $\Gamma=\mathcal{H}=\varnothing$ we set $A_{\varnothing,\varnothing}=1$. The entries in $\overleftrightarrow{A}$ for $|\Gamma|=|\mathcal{H}|=1$ can be chosen at our convenience. We will specify them such that an exact evaluation of our variational wave functions becomes feasible in infinite dimensions; see below.

After the change of the basis we obtain simple expressions for expectation values in $|\Phi_0\rangle$ with the help of Wick's theorem.[24] For example, we have

$$\begin{aligned}m^0_\Gamma&=\sum_{\mathcal{H}}|A_{\mathcal{H},\Gamma}|^2m^{h,0}_{\mathcal{H}},\\ m^{h,0}_{\mathcal{H}}&=\prod_{\boldsymbol{\sigma}\in\mathcal{H}}n^{h,0}_{\boldsymbol{\sigma}}\prod_{\boldsymbol{\sigma}\in\bar{\mathcal{H}}}(1-n^{h,0}_{\boldsymbol{\sigma}}),\end{aligned} \tag{A6}$$

where we used the fact that Fock terms are absent in the new basis; see Eq. (A3b).

2. Choice of the expansion parameter

In this subsection we suppress the site index. We proceed along the derivation outlined in Refs. 12, 13, and 20. First, we express the square of the Gutzwiller correlator $\hat{P}_G^2$ in terms of the operators for the configuration eigenstates,

$$\begin{aligned}\hat{P}^2_G&=1+\sum_\Gamma(\lambda^2_\Gamma-1)\hat{m}_\Gamma=1+\sum_{\mathcal{H},\mathcal{H}'}y_{\mathcal{H},\mathcal{H}'}\hat{m}_{\mathcal{H},\mathcal{H}'},\\ y_{\mathcal{H},\mathcal{H}'}&=\sum_\Gamma(\lambda^2_\Gamma-1)A_{\mathcal{H},\Gamma}A^+_{\Gamma,\mathcal{H}'}.\end{aligned} \tag{A7}$$

Next, we demand that

$$\sum_{\mathcal{H},\mathcal{H}'}y_{\mathcal{H},\mathcal{H}'}\hat{m}_{\mathcal{H},\mathcal{H}'}=\sum_{\mathcal{H},\mathcal{H}'(|\mathcal{H}|,|\mathcal{H}'|\geqslant 2)}x_{\mathcal{H},\mathcal{H}'}\hat{n}^{\mathrm{HF}}_{\mathcal{H},\mathcal{H}'}, \tag{A8}$$

such that

$$\hat{P}^2_G=1+\sum_{\mathcal{H},\mathcal{H}'(|\mathcal{H}|,|\mathcal{H}'|\geqslant 2)}x_{\mathcal{H},\mathcal{H}'}\hat{n}^{\mathrm{HF}}_{\mathcal{H},\mathcal{H}'}. \tag{A9}$$

Here

$$\hat{n}^{\mathrm{HF}}_{\mathcal{H},\mathcal{H}}=\hat{n}^{\mathrm{HF}}_{\mathcal{H}}=\prod_{\boldsymbol{\sigma}\in\mathcal{H}}\hat{n}^{\mathrm{HF}}_{\boldsymbol{\sigma}}, \tag{A10a}$$

$$\hat{n}^{\mathrm{HF}}_{\boldsymbol{\sigma}} = \hat{n}^{h}_{\boldsymbol{\sigma}} - n^{h,0}_{\boldsymbol{\sigma}} \tag{A10b}$$

for $\mathcal{H}=\mathcal{H}'$, and

$$\hat{n}^{\mathrm{HF}}_{\mathcal{H},\mathcal{H}'} = \left[\prod_{\boldsymbol{\sigma}\in\mathcal{J}} \hat{n}^{\mathrm{HF}}_{\boldsymbol{\sigma}}\right] \hat{n}_{\mathcal{H}_1,\mathcal{H}_2} \qquad (\mathcal{J}=\mathcal{H}\cap\mathcal{H}';\mathcal{H}=\mathcal{J}\cup\mathcal{H}_1;\mathcal{H}'=\mathcal{J}\cup\mathcal{H}_2) \tag{A10c}$$

for $\mathcal{H}\neq\mathcal{H}'$; compare Secs. II B and A 1. Note that $\langle\Phi_0|\hat{n}^{\mathrm{HF}}_{\mathcal{H}}|\Phi_0\rangle=0$ because we subtracted the Hartree terms, and all Fock terms vanish in $|\Phi_0\rangle$ due to Eq. (A3b).

The expansion of $\hat{P}^2_G$ in Eq. (A9) is chosen such that at least four lines meet at every internal vertex in our diagrammatic expansion; see below. The number of parameters $x_{\mathcal{H},\mathcal{H}'}$ in Eq. (A8) is less than the number of parameters $y_{\mathcal{H},\mathcal{H}'}$ due to the restriction $|\mathcal{H}|=|\mathcal{H}'|\geqslant 2$, i.e., we essentially require

$$x_{\varnothing,\varnothing}=0, \tag{A11a}$$

$$x_{\boldsymbol{\sigma},\boldsymbol{\sigma}'}=0. \tag{A11b}$$

Alternatively, as follows from Eq. (A9), these $1+(2N)^2$ local conditions can be formulated as

$$\langle\Phi_0|\hat{P}^2_{\mathrm{G}}|\Phi_0\rangle=1, \tag{A12a}$$

$$\langle\Phi_0|\hat{h}^{+}_{\boldsymbol{\sigma}}\hat{h}_{\boldsymbol{\sigma}'}\hat{P}^2_{\mathrm{G}}|\Phi_0\rangle=\langle\Phi_0|\hat{h}^{+}_{\boldsymbol{\sigma}}\hat{h}_{\boldsymbol{\sigma}'}|\Phi_0\rangle. \tag{A12b}$$

The first equation follows immediately because we eliminated all Hartree terms from the right-hand side of Eq. (A9). For the other $(2N)^2$ equations (A12b) we analyze the case $\boldsymbol{\sigma}=\boldsymbol{\sigma}'$ first. The operators $\hat{n}^{\mathrm{HF}}_{\mathcal{H}}$ on the right-hand side of Eq. (A9) contain at least two Hartree-Fock operators $(\hat{n}^{h}_{\boldsymbol{\sigma}_1}-n^{h,0}_{\boldsymbol{\sigma}_1})(\hat{n}^{h}_{\boldsymbol{\sigma}_2}-n^{h,0}_{\boldsymbol{\sigma}_2})$ which cannot be eliminated completely by a single operator $\hat{n}^{h}_{\boldsymbol{\sigma}}$. The term with $\hat{n}^{\mathrm{HF}}_{\mathcal{H},\mathcal{H}'}$ for $\mathcal{H}\neq\mathcal{H}'$ vanishes because of the Fock terms, which transfer electrons from $\mathcal{H}'$ to $\mathcal{H}$. According to Eq. (A3b), the expectation value of Fock terms vanishes in $|\Phi_0\rangle$. For $\boldsymbol{\sigma}\neq\boldsymbol{\sigma}'$, we note that Eq. (A10) requires $\mathcal{H}'=\boldsymbol{\gamma}\cup\boldsymbol{\sigma}$ and $\mathcal{H}=\boldsymbol{\gamma}\cup\boldsymbol{\sigma}'$ to eliminate all possible Fock terms. Nevertheless, this contribution still vanishes because of the remaining Hartree-Fock operator $\hat{n}^{\mathrm{HF}}_{\boldsymbol{\gamma}}$ for the orbital $\boldsymbol{\gamma}$. In Sec. A 6 we shall give the explicit solution of Eq. (A12) in infinite dimensions.

3. Diagrammatic theory and simplifications in infinite dimensions

Since the variational parameters obey $\lambda_{i;\Gamma}=1$ in the absence of interactions, the parameters $x_{i;\mathcal{H},\mathcal{H}'}$ go to zero for vanishing interactions. Therefore, they are suitable for a perturbation expansion in which the order of the expansion is given by the number of factors x. When we perform this expansion we may apply Wick's theorem for the resulting expectation values, since $|\Phi_0\rangle$ is a one-particle state. As usual in perturbation theory around a single-particle state,[24] the resulting contributions can be represented diagrammatically. In our theory the ''internal vertices'' represent the factors $x_{i;\mathcal{H},\mathcal{H}'}$. In addition to these internal vertices there are also ''external vertices'' which come from the site dependence of the operators $\hat{O}$. For example, there are two external vertices at the sites i and j for $\hat{O}=\hat{h}^{+}_{i;\boldsymbol{\sigma}}\hat{h}_{j;\boldsymbol{\sigma}'}$. The nontrivial result in infinite dimensions stem from the Hartree contributions at the external vertices; see below.

To obtain an expansion in powers of x, we set $\hat{P}^2_{i;G}=1+\overline{P_i}$ and write

$$\prod_i [1+\overline{P_i}] = 1+\sum_{k=1}^{\infty}\frac{1}{k!}\sum_{i_1,\ldots,i_k}{}' \prod_{j=i_1}^{i_k}\overline{P_j}, \tag{A13}$$

where $i_1,\ldots,i_k$ specify internal vertices. Here, the prime on the sum indicates that all lattice sites $i_1,\ldots,i_k$ are different when we apply Wick's theorem. Consequently, the ''lines'' of our diagrammatic theory are given by the one-particle density matrix for the single-particle wave function $|\Phi_0\rangle$ for $i\neq j$,

$$P^{\boldsymbol{\sigma},\boldsymbol{\sigma}'}_{i,j}=(1-\delta_{i,j})\langle\Phi_0|\hat{h}^{+}_{i;\boldsymbol{\sigma}}\hat{h}_{j;\boldsymbol{\sigma}'}|\Phi_0\rangle\equiv(1-\delta_{i,j})\langle\hat{h}^{+}_{i;\boldsymbol{\sigma}}\hat{h}_{j;\boldsymbol{\sigma}'}\rangle_0. \tag{A14}$$

Note that we do not have to distinguish between ''hole'' and ''particle'' lines because all sites are different when we apply Wick's theorem.[12,13,20]

To make further progress we have to apply the linked-cluster theorem.[24] Unfortunately, the restriction on the lattice sums prevents its direct application. As shown in Refs. 13 and 20, this problem can be circumvented by a redefinition of the internal vertices, i.e., $x_{i;\mathcal{H},\mathcal{H}'}\rightarrow\widetilde{x}_{i;\mathcal{H},\mathcal{H}'}$. As a result we obtain a standard diagrammatic theory with renormalized vertices $\widetilde{x}_{i;\mathcal{H},\mathcal{H}'}$ and lines given by Eq. (A14). Since the trivial order does not contain any internal vertex, it is unaffected by the redefinition of the internal vertices.

In our theory we subtracted the Hartree contributions and ruled out local Fock terms according to Eq. (A3b). For our diagrams this implies that there are no trivial loops at any internal vertex. Consequently, there are at least three independent paths from one vertex i_1 to another vertex i_2 in each nontrivial diagram, since $|\mathcal{H}|=|\mathcal{H}'|\geqslant 2$ requires that at least four lines meet at every internal vertex; paths are independent if they do not have a line in common. In the limit of infinite dimensions[9] only $i_1=i_2$ contributes to a diagram if i_1 and i_2 are linked by (at least) three independent paths. In our case this implies that the diagram simply *vanishes* since a line linking two identical vertices is zero by the definition Eq. (A14).[12,13,20] Consequently, the trivial order of our expansion gives the exact result in infinite dimension, e.g., only the diagram for $\langle\hat{h}^{+}_{i;\boldsymbol{\sigma}}\hat{h}_{j;\boldsymbol{\sigma}'}\rangle$ with a single line survives the limit $d\rightarrow\infty$. The remaining task is the calculation of the trivial (Hartree) terms which stem from the external vertices. This will be carried out for the local occupancies and the one-particle density matrix in the rest of the Appendix.

4. Local atomic occupancies

In this subsection we suppress the site index. We need to evaluate $\langle m_\Gamma\rangle$. As described in Sec. A 3, the task is readily solved in infinite dimensions,

$$m_\Gamma=\langle\hat{m}_\Gamma\rangle=\langle\hat{P}_G\hat{m}_\Gamma\hat{P}_G\rangle_0=\lambda^2_\Gamma m^0_\Gamma, \tag{A15}$$

where we used the definitions (14b) and (18). This proves Eq. (23). Furthermore, we may use this result to show that condition (A12a) is indeed fulfilled. We have

$$\langle\Phi_0|\hat{P}_G^2|\Phi_0\rangle=\left\langle\sum_\Gamma \lambda_\Gamma^2\hat{m}_\Gamma\right\rangle_0=\sum_\Gamma m_\Gamma=1, \quad \text{(A16)}$$

because the local completeness relation (14c) holds for the correlated wave function in any dimension.

For later use we write $\hat{P}_G$ in the form

$$\hat{P}_G=\sum_{\mathcal{H},\mathcal{H}'}\lambda_{\mathcal{H},\mathcal{H}'}\hat{m}_{\mathcal{H},\mathcal{H}'}, \quad \text{(A17a)}$$

where we defined

$$\lambda_{\mathcal{H},\mathcal{H}'}=\sum_\Gamma A_{\mathcal{H},\Gamma}\lambda_\Gamma A^+_{\Gamma,\mathcal{H}'}. \quad \text{(A17b)}$$

In infinite dimensions we then have

$$\begin{aligned} m_{\mathcal{H},\mathcal{H}'}&=\langle\hat{m}_{\mathcal{H},\mathcal{H}'}\rangle=\langle\hat{P}_G\hat{m}_{\mathcal{H},\mathcal{H}'}\hat{P}_G\rangle_0\\ &=\sum_{\mathcal{H}_1,\mathcal{H}_2,\mathcal{H}_3,\mathcal{H}_4}\lambda_{\mathcal{H}_1,\mathcal{H}_2}\lambda_{\mathcal{H}_3,\mathcal{H}_4}\langle\hat{m}_{\mathcal{H}_1,\mathcal{H}_2}\hat{m}_{\mathcal{H},\mathcal{H}'}\hat{m}_{\mathcal{H}_3,\mathcal{H}_4}\rangle_0\\ &=\sum_{\mathcal{K}}\lambda_{\mathcal{K},\mathcal{H}}\lambda_{\mathcal{H}',\mathcal{K}}m^{h,0}_{\mathcal{K}}, \quad \text{(A18a)}\end{aligned}$$

where we used Eq. (12) in the last step. In particular, for $\mathcal{H}=\mathcal{H}'$ we obtain

$$m_{\mathcal{H}}=m_{\mathcal{H},\mathcal{H}}=\sum_{\mathcal{K}}|\lambda_{\mathcal{K},\mathcal{H}}|^2m^{h,0}_{\mathcal{K}}. \quad \text{(A18b)}$$

With the help of Eq. (A15) and definition (A17b), Eq. (27b) follows.

Now we solve the $(2N)^2$ equations (A12b). We multiply both sides of Eq. (A9) with $\hat{h}^+_{\boldsymbol{\sigma}}\hat{h}_{\boldsymbol{\sigma}'}$, and take the expectation value with respect to $|\Phi_0\rangle$. With the help of Eqs. (14c) and (A4c), Eq. (A12b) becomes

$$\langle\hat{h}^+_{\boldsymbol{\sigma}}\hat{h}_{\boldsymbol{\sigma}'}\rangle_0=\sum_\Gamma\lambda_\Gamma^2\sum_{\mathcal{H},\mathcal{H}'}A_{\mathcal{H},\Gamma}A^+_{\Gamma,\mathcal{H}'}\langle\hat{h}^+_{\boldsymbol{\sigma}}\hat{h}_{\boldsymbol{\sigma}'}\hat{m}_{\mathcal{H},\mathcal{H}'}\rangle_0. \quad \text{(A19)}$$

Apparently we may set $\mathcal{H}=\mathcal{J}\cup\boldsymbol{\sigma}'$ $(\boldsymbol{\sigma}'\notin\mathcal{J})$. With the help of Eq. (A3b) we then find that $\mathcal{H}'=\mathcal{J}\cup\boldsymbol{\sigma}$ and, therefore, $\boldsymbol{\sigma}\notin\mathcal{J}$. We use the definition of the fermionic sign function (6) and Eq. (A15), which allow us to simplify the above equation to

$$Z_{\boldsymbol{\sigma},\boldsymbol{\sigma}'}=\sum_{|\Gamma|=1}A^*_{\boldsymbol{\sigma},\Gamma}\lambda_\Gamma^2(A^+_{\Gamma,\boldsymbol{\sigma}'})^*, \quad \text{(A20a)}$$

where the entries of the $(2N)\times(2N)$ matrix $\overleftrightarrow{Z}$ are given by

$$\begin{aligned} Z_{\boldsymbol{\sigma},\boldsymbol{\sigma}'}=&\frac{n^{h,0}_{\boldsymbol{\sigma}}}{m^{h,0}_{\boldsymbol{\sigma}}}\delta_{\boldsymbol{\sigma},\boldsymbol{\sigma}'}-\sum_{|\Gamma|\geqslant2}\frac{m_\Gamma}{m^0_\Gamma}\sum_{\mathcal{J}(\boldsymbol{\sigma},\boldsymbol{\sigma}'\notin\mathcal{J})}\mathrm{fsgn}(\boldsymbol{\sigma}',\mathcal{J})\\ &\times\mathrm{fsgn}(\boldsymbol{\sigma},\mathcal{J})A_{(\mathcal{J}\cup\boldsymbol{\sigma}'),\Gamma}A^+_{\Gamma,(\mathcal{J}\cup\boldsymbol{\sigma})}\frac{m^{h,0}_{\mathcal{J}\cup(\boldsymbol{\sigma},\boldsymbol{\sigma}')}}{m^{h,0}_{(\boldsymbol{\sigma},\boldsymbol{\sigma}')}}. \quad \text{(A20b)}\end{aligned}$$

We can safely ignore the unphysical case of $m^{h,0}_{\boldsymbol{\sigma}}=0$. All quantities in the matrix $\overleftrightarrow{Z}$ are known as soon as we fix $|\Phi_0\rangle$ and our variational parameters m_Γ for $|\Gamma|\geqslant2$. Equation (A20a) states that a unitary $(2N)\times(2N)$ matrix $\overleftrightarrow{A}'$ with $A'_{\boldsymbol{\sigma},\Gamma}\equiv A^*_{\boldsymbol{\sigma},\Gamma}$ diagonalizes the Hermitian matrix $\overleftrightarrow{Z}$, and that $\lambda^2_\Gamma\geqslant0$ $(|\Gamma|=1)$ are its eigenvalues,

$$(\overleftrightarrow{A}')^+\overleftrightarrow{Z}(\overleftrightarrow{A}')=\mathrm{diag}(\lambda^2_\Gamma). \quad \text{(A21)}$$

Therefore, conditions (A12b) fix the matrix $A_{\boldsymbol{\sigma},\Gamma}$ for $|\Gamma|=|\boldsymbol{\sigma}|=1$, and the expectation values for the atomic configurations with a single electron are given by $m_\Gamma=\lambda^2_\Gamma m^0_\Gamma$.

5. $\vec{q}$ matrix

As in Sec. A 4, we have to work in the new basis. Therefore, we start the derivation of the $\vec{q}$ matrix with a unitary transformation

$$\langle\hat{c}^+_{i;\boldsymbol{\gamma}_1}\hat{c}_{j;\boldsymbol{\gamma}'_1}\rangle=\sum_{\boldsymbol{\sigma}_1,\boldsymbol{\sigma}'_1}F_{i;\boldsymbol{\gamma}_1,\boldsymbol{\sigma}_1}F^+_{j;\boldsymbol{\sigma}'_1,\boldsymbol{\gamma}'_1}\langle\hat{h}^+_{i;\boldsymbol{\sigma}_1}\hat{h}_{j;\boldsymbol{\sigma}'_1}\rangle. \quad \text{(A22)}$$

In Sec. A 3 we showed that the calculation of the interacting one-particle density matrix reduces to

$$\langle\hat{h}^+_{i;\boldsymbol{\sigma}_1}\hat{h}_{j;\boldsymbol{\sigma}'_1}\rangle=\langle\Phi_0|(\hat{P}_{i;G}\hat{h}^+_{i;\boldsymbol{\sigma}_1}\hat{P}_{i;G})(\hat{P}_{j;G}\hat{h}_{j;\boldsymbol{\sigma}'_1}\hat{P}_{j;G})|\Phi_0\rangle \quad \text{(A23)}$$

in infinite dimensions. There we also showed that only a single line can join the two external vertices i and j. This implies

$$\langle\hat{h}^+_{i;\boldsymbol{\sigma}_1}\hat{h}_{j;\boldsymbol{\sigma}'_1}\rangle=\sum_{\boldsymbol{\sigma}_2,\boldsymbol{\sigma}'_2}\sqrt{q^{\boldsymbol{\sigma}_2}_{i;\boldsymbol{\sigma}_1}q^{\boldsymbol{\sigma}'_2}_{j;\boldsymbol{\sigma}'_1}}\langle\Phi_0|\hat{h}^+_{i;\boldsymbol{\sigma}_2}\hat{h}_{j;\boldsymbol{\sigma}'_2}|\Phi_0\rangle \quad \text{(A24a)}$$

$$\begin{aligned} &=\sum_{\boldsymbol{\gamma}_2,\boldsymbol{\gamma}'_2}\langle\hat{c}^+_{i;\boldsymbol{\gamma}_2}\hat{c}_{j;\boldsymbol{\gamma}'_2}\rangle_0\\ &\quad\times\sum_{\boldsymbol{\sigma}_2,\boldsymbol{\sigma}'_2}\sqrt{q^{\boldsymbol{\sigma}_2}_{i;\boldsymbol{\sigma}_1}q^{\boldsymbol{\sigma}'_2}_{j;\boldsymbol{\sigma}'_1}}F^+_{i;\boldsymbol{\sigma}_2,\boldsymbol{\gamma}_2}F_{j;\boldsymbol{\gamma}'_2,\boldsymbol{\sigma}'_2}, \quad \text{(A24b)}\end{aligned}$$

which proves the general structure of the variational kinetic energy (21b),

$$\langle\hat{H}_1\rangle=\sum_{i\neq j;\boldsymbol{\gamma}_1,\boldsymbol{\gamma}'_1}\tilde{t}^{\boldsymbol{\gamma}_1,\boldsymbol{\gamma}'_1}_{i,j}\langle\hat{c}^+_{i;\boldsymbol{\gamma}_1}\hat{c}_{j;\boldsymbol{\gamma}'_1}\rangle_0, \quad \text{(A25a)}$$

$$\tilde{t}_{i,j}^{\gamma_1,\gamma_1'} = \sum_{\sigma_1,\sigma_1',\sigma_2,\sigma_2'} \sqrt{q_{i;\sigma_2}^{\sigma_1} q_{j;\sigma_2'}^{\sigma_1'}} F_{i;\sigma_1,\gamma_1}^{+} F_{j;\gamma_1',\sigma_1'} \times \sum_{\gamma_2,\gamma_2'} t_{i,j}^{\gamma_2,\gamma_2'} F_{i;\gamma_2,\sigma_2} F_{j;\sigma_2',\gamma_2'}^{+}. \quad \text{(A25b)}$$

Recall that the $\overleftrightarrow{F}$ matrix is the unit matrix when Eq. (17) is fulfilled.

From now on we suppress the site index. To derive the explicit form of the $\vec{q}$ matrix we use $\hat{P}_G$ in form (A17) to write

$$\hat{P}_G \hat{h}_{\sigma}^{+} \hat{P}_G = \sum_{\mathcal{H}_1,\mathcal{H}_2,\mathcal{H}_3,\mathcal{H}_4} \lambda_{\mathcal{H}_1,\mathcal{H}_2} \lambda_{\mathcal{H}_3,\mathcal{H}_4} \hat{m}_{\mathcal{H}_1,\mathcal{H}_2} \hat{h}_{\sigma}^{+} \hat{m}_{\mathcal{H}_3,\mathcal{H}_4}. \quad \text{(A26)}$$

We use the Dirac representation of the operators $\hat{m}_{\mathcal{H},\mathcal{H}'} = |\mathcal{H}\rangle\langle\mathcal{H}'|$ and find

$$\begin{aligned}\hat{P}_G \hat{h}_{\sigma}^{+} \hat{P}_G &= \sum_{\mathcal{H}_1,\mathcal{H}_2,\mathcal{H}_3,\mathcal{H}_4} \lambda_{\mathcal{H}_1,\mathcal{H}_2} \lambda_{\mathcal{H}_3,\mathcal{H}_4} \langle \mathcal{H}_2 | \hat{h}_{\sigma}^{+} | \mathcal{H}_3 \rangle \hat{m}_{\mathcal{H}_1,\mathcal{H}_4} \\ &= \sum_{\mathcal{H}_1,\mathcal{H}_2,\mathcal{H}_3,\mathcal{H}_4} \lambda_{\mathcal{H}_1,\mathcal{H}_2} \lambda_{\mathcal{H}_3,\mathcal{H}_4} \times \mathrm{fsgn}(\sigma,\mathcal{H}_3)\, \delta_{\mathcal{H}_2,\mathcal{H}_3 \cup \sigma} \hat{m}_{\mathcal{H}_1,\mathcal{H}_4}, \end{aligned} \quad \text{(A27)}$$

where we used the definition of the fermionic sign function (6). Note that $\sigma \notin \mathcal{H}_3$ is now required. We see that $|\mathcal{H}_1| = |\mathcal{H}_4| + 1$, and our arguments presented in Sec. A 4 show that we have $\mathcal{H}_1 = \mathcal{H}' \cup \sigma'$ ($\sigma' \notin \mathcal{H}'$) and $\mathcal{H}_4 = \mathcal{H}'$ in infinite dimensions. Otherwise, local Fock terms would appear in the evaluation of Eq. (A23). For $\sigma' \notin \mathcal{H}'$ we introduce the operator

$$\hat{m}_{\mathcal{H}',\mathcal{H}'}^{\sigma'} = \prod_{\gamma \in \mathcal{H}' \setminus \sigma'} \hat{n}_{\gamma}^{h} \prod_{\gamma \in \overline{\mathcal{H}' \setminus \sigma'}} (1 - \hat{n}_{\gamma}^{h}), \quad \text{(A28)}$$

which allows us to write ($\mathcal{H}_3 \equiv \mathcal{H}$)

$$\hat{P}_G \hat{h}_{\sigma}^{+} \hat{P}_G = \sum_{\sigma'} \hat{h}_{\sigma'}^{+} \sum_{\mathcal{H}'(\sigma' \notin \mathcal{H}')} \sum_{\mathcal{H}(\sigma \notin \mathcal{H})} \times \lambda_{(\mathcal{H}' \cup \sigma'),(\mathcal{H} \cup \sigma)} \lambda_{\mathcal{H},\mathcal{H}'} \mathrm{fsgn}(\sigma,\mathcal{H}) \times \mathrm{fsgn}(\sigma',\mathcal{H}') \hat{m}_{\mathcal{H}',\mathcal{H}'}^{\sigma'} \quad \text{(A29)}$$

in infinite dimensions. When we compare this expression with Eq. (A24a), we see that

$$\sqrt{q_{\sigma}^{\sigma'}} = \sum_{\mathcal{H}'(\sigma' \notin \mathcal{H}')} \sum_{\mathcal{H}(\sigma \notin \mathcal{H})} \lambda_{(\mathcal{H}' \cup \sigma'),(\mathcal{H} \cup \sigma)} \lambda_{\mathcal{H},\mathcal{H}'} \times \mathrm{fsgn}(\sigma,\mathcal{H}) \mathrm{fsgn}(\sigma',\mathcal{H}') \langle \hat{m}_{\mathcal{H}',\mathcal{H}'}^{\sigma'} \rangle_0, \quad \text{(A30)}$$

because we finally singled out the electron creation operator $\hat{h}_{\sigma'}^{+}$ for the contraction according to Wick's theorem in Eq. (A24a). We use Eqs. (A15) and (A17b) and the trivial relation

$$\langle \hat{m}_{\mathcal{H}',\mathcal{H}'}^{\sigma'} \rangle_0 = \frac{m_{\mathcal{H}'}^{h,0}}{1 - n_{\sigma'}^{h,0}} = \sqrt{\frac{m_{\mathcal{H}'}^{h,0} m_{(\mathcal{H}' \cup \sigma')}^{h,0}}{n_{\sigma'}^{h,0}(1 - n_{\sigma'}^{h,0})}} \quad \text{(A31)}$$

to derive the $\vec{q}$ matrix in the form

$$\begin{aligned}\sqrt{q_{\sigma}^{\sigma'}} = \sqrt{\frac{1}{n_{\sigma'}^{h,0}(1 - n_{\sigma'}^{h,0})}} \sum_{\Gamma,\Gamma'} \sqrt{\frac{m_{\Gamma} m_{\Gamma'}}{m_{\Gamma}^{0} m_{\Gamma'}^{0}}} \\ \times \sum_{\substack{\mathcal{H},\mathcal{H}' \\ (\sigma \notin \mathcal{H}, \sigma' \notin \mathcal{H}')}} \mathrm{fsgn}(\sigma',\mathcal{H}') \mathrm{fsgn}(\sigma,\mathcal{H}) \\ \times \sqrt{m_{(\mathcal{H}' \cup \sigma')}^{h,0} m_{\mathcal{H}'}^{h,0}} A_{\Gamma,(\mathcal{H} \cup \sigma)}^{+} A_{(\mathcal{H}' \cup \sigma'),\Gamma} A_{\Gamma',\mathcal{H}'}^{+} A_{\mathcal{H},\Gamma'}. \end{aligned} \quad \text{(A32)}$$

When Eq. (17) holds, we recover Eq. (22).

6. Local one-particle density matrix

Finally, we derive an expression for the *interacting* local one-particle density matrix,

$$C_{\gamma_1,\gamma_1'} = \langle \hat{c}_{\gamma_1}^{+} \hat{c}_{\gamma_1'} \rangle. \quad \text{(A33a)}$$

Note that the local gross occupancies are the diagonal entries of this matrix, $n_{\gamma} = C_{\gamma,\gamma}$. We express this matrix in the new basis,

$$C_{\gamma_1,\gamma_1'} = \sum_{\sigma_1,\sigma_1'} F_{\gamma_1,\sigma_1} F_{\sigma_1',\gamma_1'}^{+} \langle \hat{h}_{\sigma_1}^{+} \hat{h}_{\sigma_1'} \rangle. \quad \text{(A33b)}$$

In infinite dimensions the entries of the interacting local one-particle density matrix $\overleftrightarrow{H}$ in the new basis are readily calculated,

$$\begin{aligned} H_{\sigma_1,\sigma_1'} &= \langle \hat{h}_{\sigma_1}^{+} \hat{h}_{\sigma_1'} \rangle = \langle \hat{P}_G \hat{h}_{\sigma_1}^{+} \hat{h}_{\sigma_1'} \hat{P}_G \rangle_0 \\ &= \sum_{\mathcal{H}_1,\mathcal{H}_2,\mathcal{H}_3,\mathcal{H}_4} \lambda_{\mathcal{H}_1,\mathcal{H}_2} \lambda_{\mathcal{H}_3,\mathcal{H}_4} \times \langle \hat{m}_{\mathcal{H}_1,\mathcal{H}_2} \hat{h}_{\sigma_1}^{+} \hat{h}_{\sigma_1'} \hat{m}_{\mathcal{H}_3,\mathcal{H}_4} \rangle_0. \end{aligned} \quad \text{(A34)}$$

In infinite dimensions we may set $\mathcal{H}_1 = \mathcal{H}_4 = \mathcal{H}'$, $\mathcal{H}_3 = \mathcal{H} \cup \sigma_1'$, and $\mathcal{H}_2 = \mathcal{H} \cup \sigma_1$ with $\sigma_1, \sigma_1' \notin \mathcal{H}$. We then find

$$H_{\boldsymbol{\sigma}_1,\boldsymbol{\sigma}_1'} = \sum_{\substack{\mathcal{H} \\ (\boldsymbol{\sigma}_1,\boldsymbol{\sigma}_1' \notin \mathcal{H})}} \mathrm{fsgn}(\boldsymbol{\sigma}_1,\mathcal{H})\,\mathrm{fsgn}(\boldsymbol{\sigma}_1',\mathcal{H}) \times \sum_{\mathcal{H}'} \lambda_{\mathcal{H}',\mathcal{H}\cup\boldsymbol{\sigma}_1}\lambda_{\mathcal{H}\cup\boldsymbol{\sigma}_1',\mathcal{H}'} m^{h,0}_{\mathcal{H}'}$$

$$= \sum_{\substack{\mathcal{H} \\ (\boldsymbol{\sigma}_1,\boldsymbol{\sigma}_1' \notin \mathcal{H})}} \mathrm{fsgn}(\boldsymbol{\sigma}_1,\mathcal{H})\,\mathrm{fsgn}(\boldsymbol{\sigma}_1',\mathcal{H}) \times \sum_{\Gamma,\Gamma'} \sqrt{\frac{m_\Gamma m_{\Gamma'}}{m^0_\Gamma m^0_{\Gamma'}}} A^+_{\Gamma,\mathcal{H}\cup\boldsymbol{\sigma}_1} A_{\mathcal{H}\cup\boldsymbol{\sigma}_1',\Gamma'} \times \sum_{\mathcal{H}'} A_{\mathcal{H}',\Gamma} A^+_{\Gamma',\mathcal{H}'} m^{h,0}_{\mathcal{H}'}. \quad \text{(A35)}$$

Therefore, the matrix $\overleftrightarrow{H}$ is known in terms of the variational parameters m_Γ and the properties of the one-particle product state $|\Phi_0\rangle$. If the noninteracting local-density matrix $\overleftrightarrow{C}^0$ is diagonal, i.e., Eq. (17) is fulfilled, the matrices $\overleftrightarrow{C}$ and $\overleftrightarrow{H}$ are identical, and Eq. (A35) also leads to Eq. (27). The matrix $\overleftrightarrow{H}$ is Hermitian and can thus be diagonalized with the help of the unitary matrix $\overleftrightarrow{X}$,

$$(\overleftrightarrow{X})^+ \overleftrightarrow{H} \overleftrightarrow{X} = \mathrm{diag}(\tilde{n}^h_{\boldsymbol{\sigma}}), \quad \text{(A36)}$$

where $\tilde{n}^h_{\boldsymbol{\sigma}}$ are the eigenvalues of the matrix $\overleftrightarrow{H}$. The entries of $\overleftrightarrow{H}$ thus obey

$$H_{\boldsymbol{\sigma}_1,\boldsymbol{\sigma}_1'} = \sum_{\boldsymbol{\sigma}_2,\boldsymbol{\sigma}_2'} X_{\boldsymbol{\sigma}_1,\boldsymbol{\sigma}_2}\delta_{\boldsymbol{\sigma}_2,\boldsymbol{\sigma}_2'}\tilde{n}^h_{\boldsymbol{\sigma}_2} X^+_{\boldsymbol{\sigma}_2',\boldsymbol{\sigma}_1'} = \sum_{\boldsymbol{\sigma}_2,\boldsymbol{\sigma}_2'} X_{\boldsymbol{\sigma}_1,\boldsymbol{\sigma}_2} \frac{\tilde{n}^h_{\boldsymbol{\sigma}_2}}{n^{h,0}_{\boldsymbol{\sigma}_2}} \langle \hat{h}^+_{\boldsymbol{\sigma}_2}\hat{h}_{\boldsymbol{\sigma}_2'}\rangle_0 X^+_{\boldsymbol{\sigma}_2',\boldsymbol{\sigma}_1'}. \quad \text{(A37)}$$

We transform back into the representation with $\hat{c}$ operators and find for the interacting local one-particle density matrix in the original basis

$$C_{\gamma_1,\gamma_1'} = \sum_{\gamma_2,\gamma_2'} C^0_{\gamma_2,\gamma_2'} \sum_{\boldsymbol{\sigma}_1,\boldsymbol{\sigma}_1',\boldsymbol{\sigma}_2,\boldsymbol{\sigma}_2'} F^+_{\boldsymbol{\sigma}_2,\gamma_2} F_{\gamma_2',\boldsymbol{\sigma}_2'} X_{\boldsymbol{\sigma}_1,\boldsymbol{\sigma}_2} \times \frac{\tilde{n}^h_{\boldsymbol{\sigma}_2}}{n^{h,0}_{\boldsymbol{\sigma}_2}} X^+_{\boldsymbol{\sigma}_2',\boldsymbol{\sigma}_1'} F_{\gamma_1,\boldsymbol{\sigma}_1} F^+_{\boldsymbol{\sigma}_1',\gamma_1'}. \quad \text{(A38)}$$

Recall that the local gross occupancies are the diagonal entries of this matrix, $n_\gamma = C_{\gamma,\gamma}$.

The result (A38) allows us to cast the local hybridization term in the variational ground-state energy into the form

$$\sum_{\gamma_1,\gamma_1'} t^{\gamma_1,\gamma_1'} \langle \hat{c}^+_{\gamma_1}\hat{c}_{\gamma_1'}\rangle = \sum_{\gamma_2,\gamma_2'} \tilde{t}^{\gamma_2,\gamma_2'} \langle \hat{c}^+_{\gamma_2}\hat{c}_{\gamma_2'}\rangle_0, \quad \text{(A39a)}$$

where the effective local hybridizations are given by

$$\tilde{t}^{\gamma_2,\gamma_2'} = \sum_{\gamma_1,\gamma_1'} t^{\gamma_1,\gamma_1'} \sum_{\boldsymbol{\sigma}_1,\boldsymbol{\sigma}_1'} F_{\gamma_1,\boldsymbol{\sigma}_1} F^+_{\boldsymbol{\sigma}_1',\gamma_1'} \sum_{\boldsymbol{\sigma}_2,\boldsymbol{\sigma}_2'} X_{\boldsymbol{\sigma}_1,\boldsymbol{\sigma}_2} \times \frac{\tilde{n}^h_{\boldsymbol{\sigma}_2}}{n^{h,0}_{\boldsymbol{\sigma}_2}} X^+_{\boldsymbol{\sigma}_2',\boldsymbol{\sigma}_1'} F^+_{\boldsymbol{\sigma}_2,\gamma_2} F_{\gamma_2',\boldsymbol{\sigma}_2'}. \quad \text{(A39b)}$$

This expression simplifies if we assume that there are no local Fock terms already in the basis of the $\hat{c}$ operators. Then the $\overleftrightarrow{F}$ matrix becomes the unit matrix. Let us further demand that orbitals with different crystal-field energies do not mix, i.e., $t^{\gamma,\gamma'} = \delta_{\gamma,\gamma'}\epsilon_\gamma$. If our one-particle product state $|\Phi_0\rangle$ respects this symmetry, the $\overleftrightarrow{X}$ matrix becomes the unit matrix, and we find

$$\tilde{t}^{\gamma_2,\gamma_2'} = \delta_{\gamma_2,\gamma_2'}\epsilon_{\gamma_2}\frac{n_{\gamma_2}}{n^0_{\gamma_2}}. \quad \text{(A40)}$$

Thus we recover Eq. (28b) for the effective crystal-field energies.

[1] J. H. van Vleck, Rev. Mod. Phys. **25**, 220 (1953); for a general introduction, see C. Herring in *Magnetism*, edited by G. T. Rado and H. Suhl (Academic, New York, 1966), Vol. IV, p. 1.

[2] V. R. Moruzzi, J. F. Janak, and A. R. Williams, *Calculated Properties of Metals* (Pergamon, New York, 1978).

[3] M. C. Gutzwiller, Phys. Rev. Lett. **10**, 159 (1963); Phys. Rev. **134**, A923 (1964); **137**, A1726 (1965).

[4] J. Hubbard, Proc. R. Soc. London, Ser. A **276**, 238 (1963); **277**, 237 (1964); **281**, 401 (1964).

[5] W. F. Brinkman and T. M. Rice, Phys. Rev. B **2**, 4302 (1970).

[6] N. F. Mott, *Metal-Insulator Transitions*, 2nd ed. (Taylor and Francis, London, 1990).

[7] F. Gebhard, *The Mott Metal-Insulator Transition—Models and Methods*, Springer Tracts in Modern Physics Vol. 137 (Springer, Berlin, 1997).

[8] W. Metzner and D. Vollhardt, Phys. Rev. Lett. **59**, 121 (1987); Phys. Rev. B **37**, 7382 (1988); F. Gebhard and D. Vollhardt, Phys. Rev. Lett. **59**, 1472 (1987); Phys. Rev. B **38**, 6911 (1988).

[9] W. Metzner and D. Vollhardt, Phys. Rev. Lett. **62**, 324 (1989).

[10] W. Metzner, Z. Phys. B **77**, 253 (1989).

[11] G. Kotliar and A. E. Ruckenstein, Phys. Rev. Lett. **57**, 1362 (1986).

[12] F. Gebhard, Phys. Rev. B **41**, 9452 (1990).

[13] F. Gebhard, Phys. Rev. B **44**, 992 (1991).

[14] P. Coleman, Phys. Rev. B **28**, 5255 (1983); **29**, 3035 (1984); **35**, 5072 (1987); N. Read and D. M. Newns, J. Phys. C **16**, 3273 (1983); Adv. Phys. **36**, 799 (1987).

[15] P. Fulde, *Electron Correlations in Molecules and Solids*, Springer Series in Solid-State Sciences Vol. 100 (Springer, Berlin, 1991).

[16] G. Stollhoff and P. Fulde, J. Chem. Phys. **73**, 4548 (1980); G.

Stollhoff and P. Thalmeier, Z. Phys. B **43**, 13 (1981); A. M. Oleś and G. Stollhoff, Phys. Rev. B **29**, 314 (1984).
[17] J. Bünemann and W. Weber, Phys. Rev. B **55**, 4011 (1997).
[18] J. Bünemann and W. Weber, Physica B **230-232**, 412 (1997).
[19] T. Okabe, J. Phys. Soc. Jpn. **65**, 1056 (1996).
[20] J. Bünemann, F. Gebhard, and W. Weber, J. Phys.: Condens. Matter **8**, 7343 (1997).
[21] J. S. Griffith, *The Theory of Transition-Metal Ions* (Cambridge University Press, Cambridge, 1964).
[22] C. J. Ballhausen, *Introduction to Ligand Field Theory* (McGraw-Hill, New York, 1962).
[23] S. Sugano, Y. Tanabe, and H. Kamimura, *Multiplets of Transition-Metal Ions in Crystals*, Pure and Applied Physics Vol. 33 (Academic, New York, 1970).
[24] A. L. Fetter and J. D. Walecka, *Quantum Theory of Many-Particle Systems* (McGraw-Hill, New York, 1971).
[25] D. Vollhardt, in *Correlated Electron Systems*, edited by V. J. Emery (World Scientific, Singapore, 1993), Vol. 9, p. 57; Int. J. Mod. Phys. B **3**, 2189 (1989).
[26] A. Georges, G. Kotliar, W. Krauth, and M. J. Rozenberg, Rev. Mod. Phys. **68**, 13 (1996).
[27] D. Vollhardt, Rev. Mod. Phys. **56**, 99 (1984).
[28] D. Pines and P. Nozières, *The Theory of Quantum Liquids*, 2nd ed. (Addison-Wesley, New York, 1988).
[29] A. J. Leggett, Rev. Mod. Phys. **47**, 331 (1975).
[30] J. Bünemann, (unpublished).
[31] In Ref. 20 we used the notation $\eta_{i;I}$ instead of $g_{i;I}$ for $|I|\leqslant 1$. In Ref. 12 the notation $g^{-\mu_{i;\uparrow}}\equiv g_{i;\uparrow}$, $g^{-\mu_{i;\downarrow}}\equiv g_{i;\uparrow}$, and $g^{\eta_i}\equiv g_{i;\varnothing}$ was used.
[32] H. Hasegawa, J. Phys. Soc. Jpn. **66**, 1391 (1997); Phys. Rev. B **56**, 1196 (1997).
[33] R. Frésard and G. Kotliar, Phys. Rev. B **56**, 12 909 (1997).
[34] V. Dorin and P. Schlottmann, Phys. Rev. B **47**, 5095 (1995).
[35] H. Yokoyama and H. Shiba, J. Phys. Soc. Jpn. **56**, 1490 (1987); **56**, 3570 (1987); **56**, 3582 (1987).
[36] J. C. Slater and G. F. Koster, Phys. Rev. **94**, 1498 (1954).
[37] P. G. J. van Dongen, F. Gebhard, and D. Vollhardt, Z. Phys. B **76**, 199 (1989).
[38] P. Fazekas, B. Menge, and E. Müller-Hartmann, Z. Phys. B **78**, 69 (1990).
[39] J. P. Lu, Phys. Rev. B **49**, 5687 (1994); Int. J. Mod. Phys. B **10**, 3717 (1996).